Review

Open Access Data in Polar and Cryospheric Remote Sensing

Allen Pope [1,2,3,*], W. Gareth Rees [3], Adrian J. Fox [4] and Andrew Fleming [4]

[1] National Snow and Ice Data Center, University of Colorado, 1540 30th Street, Boulder, CO 80303, USA

[2] Earth Science Department, HB 6105 Fairchild Hall, Dartmouth College, Hanover, NH 03755, USA

[3] Scott Polar Research Institute, University of Cambridge, Lensfield Road, Cambridge CB2 1ER, UK; E-Mail: wgr2@cam.ac.uk

[4] British Antarctic Survey, High Cross, Madingley Road, Cambridge CB3 0ET, UK; E-Mails: ajfo@bas.ac.uk (A.J.F.); ahf@bas.ac.uk (A.F.)

* Author to whom correspondence should be addressed; E-Mail: allen.pope@nsidc.org; Tel.: +1-303-492-9077; Fax: +1-303-492-2468.

Abstract: This paper aims to introduce the main types and sources of remotely sensed data that are freely available and have cryospheric applications. We describe aerial and satellite photography, satellite-borne visible, near-infrared and thermal infrared sensors, synthetic aperture radar, passive microwave imagers and active microwave scatterometers. We consider the availability and practical utility of archival data, dating back in some cases to the 1920s for aerial photography and the 1960s for satellite imagery, the data that are being collected today and the prospects for future data collection; in all cases, with a focus on data that are openly accessible. Derived data products are increasingly available, and we give examples of such products of particular value in polar and cryospheric research. We also discuss the availability and applicability of free and, where possible, open-source software tools for reading and processing remotely sensed data. The paper concludes with a discussion of open data access within polar and cryospheric sciences, considering trends in data discoverability, access, sharing and use.

1. Introduction

In many fields, changes influencing polar and cryospheric environments have proven to have global impacts. Earth observation and remote sensing tools are well-suited to applications in polar and cryospheric research, allowing observations at lower initial cost to the researcher, higher frequency and at a synoptic scale complementary to *in situ* measurements. Whether studying glacier extent and behavior, ice sheet activity, sea ice extent, lake and river ice, snow cover extent and water equivalent, ocean circulation, tree line migration, permafrost lake dynamics, circumpolar environmental impact assessment or penguin populations, recent research has clearly demonstrated the increasing importance of Earth observation. Nevertheless, many products and sources of data are restricted or highly priced.

Encouragingly, as highlighted in the Antarctic Treaty, a SCAR (Scientific Committee on Antarctic Research) standing resolution and the 2007–2009 International Polar Year [1], polar research has made clear the importance of open data access, archiving and sharing between research programs. Indeed, many remote sensing data providers also espouse the ethos of free and open access to quality data sets in order to enable researchers to pursue experimental, interdisciplinary, international and innovative Earth observation research economically. Remote sensing data are often provided by (inter)governmental agencies, which can streamline the ability to provide data in a coordinated fashion. As a prominent example, the Landsat program has revolutionized the use of its data through a new data policy [2].

Recently, rapid developments in web tools, storage space, Internet bandwidth and the availability of computing resources have changed the remote sensing landscape. The challenge has moved from obtaining any data at all to identifying high-quality data fit for addressing a particular research question.

Therefore, the aims of this paper are to provide a review of primary open access remote sensing data sources, products and tools and to discuss the opening of data access in polar and cryospheric remote sensing. This can serve as a primer for students, for polar scientists new to remote sensing or remote sensing specialists new to polar science. In a time of tightening budgets and opening research, this article will, to the best of the authors' capabilities, describe the developments of different types of data (multispectral imagery, synthetic aperture radar, passive microwave data, active microwave scatterometry and others), provide some references for follow-up and point towards raw data, products, and tools to manipulate data, which are all openly available.

2. Historical Data

There is significant interest and scientific value in reconstructing past landscapes. In some disciplines, that means going to the geological record or to ice cores. In remote sensing, it means looking back to the middle of the 20th century and rescuing data that have since been relegated to reels and tapes or collected by analog systems. Much early remote sensing data were acquired for regional reconnaissance, mapping and charting, not science. Thus, a large scientific hurdle to overcome is that of sparse coverage. We can only work with what was acquired at the time and devise experimental methods to unlock the available data. To add to this challenge, metadata and image quality problems can provide challenges for quantitative use. Still, with patience and innovation, historical data can be an untapped resource for understanding environmental change over recent decades.

2.1. Aerial Photography in the Polar Regions

The initial impetus for early aerial photography (or airphot) of the polar regions was strategic topographic mapping by national mapping agencies. For regional, strategic mapping programs, the focus was on systematically covering large geographical areas as efficiently as possible. Therefore, oblique aerial photography was commonly used, especially for what was really reconnaissance mapping of largely unknown areas.

Following further developments in aviation, photography and plotting techniques driven by reconnaissance and military mapping during World War II (WWII), topographic mapping from vertical aerial photography became the norm. National mapping and military agencies began to acquire systematic coverage of polar regions, initially often using ex-military cameras from the WWII era. Some of this aerial photography was acquired using near-infrared film, originally developed for military use as camouflage detection film; this preserves a record of vegetation coverage at the time.

Large areas of both the Arctic and Antarctica were covered by aerial photography flown by the U.S. Army Map Service in the late 1940s and 1950s as part of Cold War strategic information gathering. The value today of this legacy of hundreds of thousands of historic aerial photographs for studying environmental changes is incidental to the original reconnaissance and topographic mapping purpose; photos provide a baseline for environmental variables purely because these features happen to be part of the topography.

Following WWII, there was separately an intentional effort to use aerial photography for Arctic and lower-latitude glacier monitoring. Regular measurements of mass-balance for selected glaciers in Scandinavia, the Alps, Alaska and the former Soviet Union, some of which continue to this day, were initiated in the 1940s [3]. Some of these selected glaciers also have an archive of repeat coverage, even though there may not be regional coverage with the same frequency.

While these glaciers were targeted for monitoring studies, the majority of polar aerial photography did not have a scientific focus. As a consequence, the photographs can often be difficult to use quantitatively for detailed studies and are an under-utilized resource. Flight lines are usually aligned for efficient regional coverage rather than optimally for landscape features, for example along the central flow-line of a glacier. In the decades since the aerial photographs were acquired, some datasets have lost metadata about the cameras and lenses that were used, which hinders precise photogrammetric work. Additionally, remote polar areas often have geodetic survey networks that are too sparse to accurately georeference the photography, and acquiring adequate ground control points is difficult and expensive for large areas in accessible regions.

Fortunately, applying modern photogrammetry and image analysis methods can overcome these problems, unlocking the legacy of aerial photographs for detailed measurements of landscape change over decadal scales. For example, some studies have used calibration from military cartographic cameras [4,5] and linking or surface matching to modern satellite or airborne images to improve measurements of historic glacier volume change on the Antarctic Peninsula [6,7]. Others use modern GPS or LiDAR data to fix ground control points in historical photos for photogrammetric processing [8–10]. These new techniques and ancillary data can bring new life to historical remote sensing data.

Analogue aerial photographs from a half-century ago cannot match the resolution and radiometric depth of modern digital camera systems and can have problems with image saturation and lack of surface detail on snow surfaces. Nevertheless, aerial photography camera, lens and film technologies were evolving rapidly during the 1950s and 1960s, and aerial photographs from this period that have been well stored can be of surprisingly high quality. Image-enhancement tools in modern photogrammetry software can maximize the extraction of subtle surface features from scanned analogue aerial photographs.

2.1.1. The Arctic

This section is a concise summary of aerial photography coverage for various regions in the Arctic. Note, the listings are limited to areas where data are known to be available, which will limit the coverage in some regions (e.g., Arctic Russia).

Norway/Svalbard: Norway compiled a series of 1:100,000 scale maps of Svalbard from 1936 onwards, beginning with oblique photography acquired in 1936, 1938 and 1956. Vertical aerial photography campaigns at 1:50,000 scale in the 1960s and 1970s, notably 1966, when almost complete coverage was achieved, ensured that all areas were covered at least once by the 1970s. There is almost complete systematic coverage at 1:50,000 scale with color infrared (CIR) film acquired in 1990 and further photography from 1995 and 2000 for selected areas [11,12].

Similarly, aerial photography was being flown for topographic mapping on the Norwegian mainland, including systematic photography of the Norway/Sweden border in 1957 (http://www.norgeibilder.no/).

Iceland: Systematic topographic map compilation from aerial photography for Iceland began in 1937 from oblique photos flown in 1937 and 1938 [13,14]. Earlier mapping efforts were then superseded by 1:50,000 scale maps with more accurate contours on glaciers in 1948–1949, produced by the U.S. Army Map Service from vertical aerial photography flown in 1946–1947.

Greenland: In Greenland, parts of the east coast had been mapped from aerial photography as early as 1937, with much mapping activity in the late 1940s and 1950s, and the far north was mapped after WWII by the U.S. Army Map Service [15]. Aerial photography cover for accurate topographic mapping of even the ice-free areas in north Greenland was not completed until a campaign by the Danish Geodetic Institute in 1978, with mapping beginning in the 1980s. In addition, oblique aerial photos from Greenland expeditions are available from collections in Denmark, at the Scott Polar Research Institute in Cambridge and elsewhere and have been used to reconstruct, for example, 80 years of glacier change in southeast Greenland [16].

Canadian Arctic and Alaska: Due to the technical challenges of dealing with vast remote areas, national mapping agencies did not undertake extensive aerial photography of the Western hemisphere Arctic (Alaska and Canada) until the 1950s, following further developments in aviation and photogrammetric techniques, particularly aerotriangulation, to deal with the vast geographic areas involved [17–20].

The Alaska High Altitude Photography (AHAP) collection, 1978–1986, covers about 95% of the State of Alaska in both 1:60,000 CIR and 1:120,000 black and white photography. Approximately 60,000 frames of photography have been scanned by the USGS EROS data center at medium

resolution (400 dpi). Imagery and metadata are available from the Polar Geospatial Center (PGC; http://www.pgc.umn.edu/imagery/aerial).

In addition, over six million aerial photographs over Canada are available for a nominal fee from the National Air Photo Library (NAPL) of Natural Resources Canada. The metadata are freely available and searchable at http://www.nrcan.gc.ca/earth-sciences/geomatics/satellite-imagery-air-photos/9265. There are also a large number of freely available photographs of Alaskan and Canadian glaciers in the Glacier Photograph Collection (https://nsidc.org/data/glacier_photo/) [21].

2.1.2. The Antarctic Peninsula

The Antarctic Peninsula has the best aerial photography coverage on the Antarctic continent. Much of this was completed under the auspices of the U.K. Royal Navy, the British Antarctic Survey and its predecessors (see Table 1). Beyond the Peninsula, U.S. reconnaissance did span much of the wider continent. Additionally, other countries (e.g., Germany, Norway) completed smaller regional surveys, often attached to Antarctic territorial claims. For this reason, although significant international coverage is present on the Peninsula, there are many regions on the continent with solely U.S. coverage.

The earliest aerial photography in the Antarctic Peninsula was flown by private expeditions led by Hubert Wilkins (1928–1930) and Lincoln Ellsworth (1935) and by the British Graham Land Expedition (1934–1937). The oblique aerial photographs yielded much valuable information, but were not used for rigorous mapping.

The first aerial survey sortie took place on the German Antarctic Expedition of 1938–1939 in Neuschwabenland, as part of making a territorial claim for Germany. The photographs were used for mapping by Otto Von Gruber in 1942.

The first extensive aerial photography coverage was acquired by the Ronne Antarctic Research Expedition (RARE) in 1947 using Fairchild T2 Trimetrogon cameras. Trimetrogon photography uses three cameras (vertical and left- and right-looking obliques) to give horizon-to-horizon coverage. The image quality is very high for these photographs, but they are difficult to use for photogrammetry. They were flown in long exploratory flight lines rather than for systematic coverage, and only the vertical photography component of the Trimetrogon arrangement is suitable for accurate, rather than reconnaissance, topographic mapping applications. Unfortunately, the negatives and calibration metadata have been lost, and the lenses in these cameras typically have high distortion levels [4].

The Falkland Islands Dependencies Aerial Survey Expedition (FIDASE) 1956–1957 acquired the first systematic vertical aerial photography and ground survey for photogrammetry for the northwest part of the Antarctic Peninsula [22,23]. The photography was flown at a usual altitude of 13,500 feet and was planned for photogrammetric mapping with 60% overlap and 15% sidelap; imagery has been scanned and is digitally available through the United States Geological Survey (USGS; https://earthexplorer.usgs.gov/). The photography was used for 1:200,000 and 1:250,000 scale topographic mapping by the U.K. Department of Overseas Surveys (DOS) throughout the 1960s and 1970s (e.g., [24]). This extensive campaign remains the largest attempt at systematic regional coverage of vertical, photogrammetric quality aerial photography coverage and is still the best available aerial photography for large areas of the Antarctic Peninsula. These DOS maps are still the only systematic photogrammetric mapping scheme for the Antarctic Peninsula, but unfortunately, only coverage of the

Peninsula to 68°S was completed. The maps were a great advance over previous mapping, which was based on plane-tabling and surveyors' sketches on overland traverses. However, the small scale and the large contour interval (100 m) severely restrict their usefulness as a record of the glacier surfaces, and the accuracy of the photogrammetry is not quantified.

During the late 1960s, the U.S. Air Force and U.S. Navy carried out extensive Trimetrogon aerial photography coverage of large parts of Antarctica, including the Antarctic Peninsula, as the basis for a series of reconnaissance maps at 1:250,000 scale. This photography is known as Trimetrogon Antarctica (TMA). It was flown more systematically than the RARE Trimetrogon photography, but still has the constraints of only the vertical segment being suitable for highly accurate work and the use of metrogon lenses. Whilst the negatives are still available, some of the metadata about individual sorties have also been lost. Nevertheless, over 330,000 photos were scanned by the United States Geological Survey and are available with flight lines through the Polar Geospatial Center (http://www.pgc.umn.edu/imagery/aerial/antarctica).

Since the TMA campaigns in the 1960s, vertical aerial photography on the Antarctic Peninsula has been carried out by both the Royal Navy (RN) and the British Antarctic Survey (BAS). The RN photography was acquired to support hydrographic charting and is usually single strips of photographs following the coastline. The BAS photography has always been flown to support specific projects, rather than for systematic regional coverage, and the coverage is patchy. The majority of the RN and BAS coverage was acquired using high quality Zeiss or Leica metric cameras, but there is also some BAS photography using a Vinten medium format reconnaissance camera.

In 1989, the German Institut für Angewandte Geodäsie (IfAG), in collaboration with BAS, acquired systematic coverage of the Marguerite Bay area, on the west side of the Antarctic Peninsula, at 1:70,000 scale. This photography has been used for rigorous photogrammetric mapping of selected areas by BAS, as well as the University of Darmstadt, Germany [25].

Table 1. Summary of Antarctic Peninsula aerial photography campaigns. FIDASE, Falkland Islands Dependencies Aerial Survey; TMA, Trimetrogon Antarctica; BAS, British Antarctic Survey; IfAG, Expedition Institut für Angewandte Geodäsie.

Year	Aerial Photography Type
1947	Ronne Antarctic Research Expedition (vertical and oblique)
1956–1957	FIDASE (vertical 1:27,000)
1964–1969	U.S. Navy TMA Trimetrogon (vertical 1:38,000 and oblique)
1972–1979, 1986, 1989, 1990–2002	British Royal Navy (vertical 1:12,000; 1:24,000)
1962, 1986, 1989–2005	BAS (vertical 1:20,000 to 1:30,000), some medium format vertical
1989	IfAG (vertical 1:70,000)

## 2.2. Satellite Photography and Multispectral Imaging

Innovations in films, lenses and aerospace engineering enabled the next generation of surveillance: satellite photography. These sensors next evolved into multispectral imagers, isolating different spectral components of each image to collect data in multiple bands and expanding the knowledge about the surface that was being imaged. The basics of remote sensing are beyond the scope of this

article, and for subject-specific technical treatment of remote sensing theory and definitions, readers are directed to available textbooks (e.g., [26,27]) and appropriate review articles (e.g., [28–31]).

Declassified surveillance imagery has enabled the change record to be pushed back by decades, especially in regions of strategic interest to the United States, including extensive areas in the Arctic, Antarctic and mountain areas, such as the Himalayas (e.g., [32,33]). Declassified images from the Argon, Corona, Gambit, Hexagon and Lanyard (collectively known as Keyhole) Programs are online, covering dates ranging from 1960 to 1980 and with ground resolutions available under a meter for some images; although there is a small processing charge (currently 30 USD) for the first request to access a high-resolution archived image, subsequent downloads are free to all users (http://earthexplorer.usgs.gov/). In addition, a "fiducial" (*i.e.*, reference) dataset of declassified meter-scale imagery of polar areas is available with coverage beginning in 1999. Some coverage is at fixed sites in the Antarctic (various sites in the Dry Valleys and Palmer Station; http://gfl.usgs.gov/site_info_antarctica.shtml?current=3) and sea ice areas in the Arctic Basin (designated Beaufort, Canadian Arctic, Fram, Siberia, Chukchi and Barrow), while coverage of floating buoys began in 2009 (http://gfl.usgs.gov/site_info_arctic_sea.shtml?current=2) [34].

Multispectral imagery has an enormous range of applications in circumpolar and cryospheric environments. There are many different available sensors (see Figure 1), offering a wide range of combinations of spatial resolution, revisit time, radiometric sensitivity, imaging bands, scene size, processed products, coverage area and data archive. It is therefore important to use these variables to choose the optimum sensor for a particular application.

Figure 1. Historical, ongoing and future satellite optical and multispectral sensors (with platforms in parentheses) with some or all freely available data. Mission-specific details: the hatched period for ETM+/Landsat 7 indicates the SLC-off period and the gray section of the fiducial dataset indicates when only fixed-site imagery is available; beginning in 2009, images of both fixed sites' floating buoys are available. VIIRS, Visible Infrared Imaging Radiometer Suite.
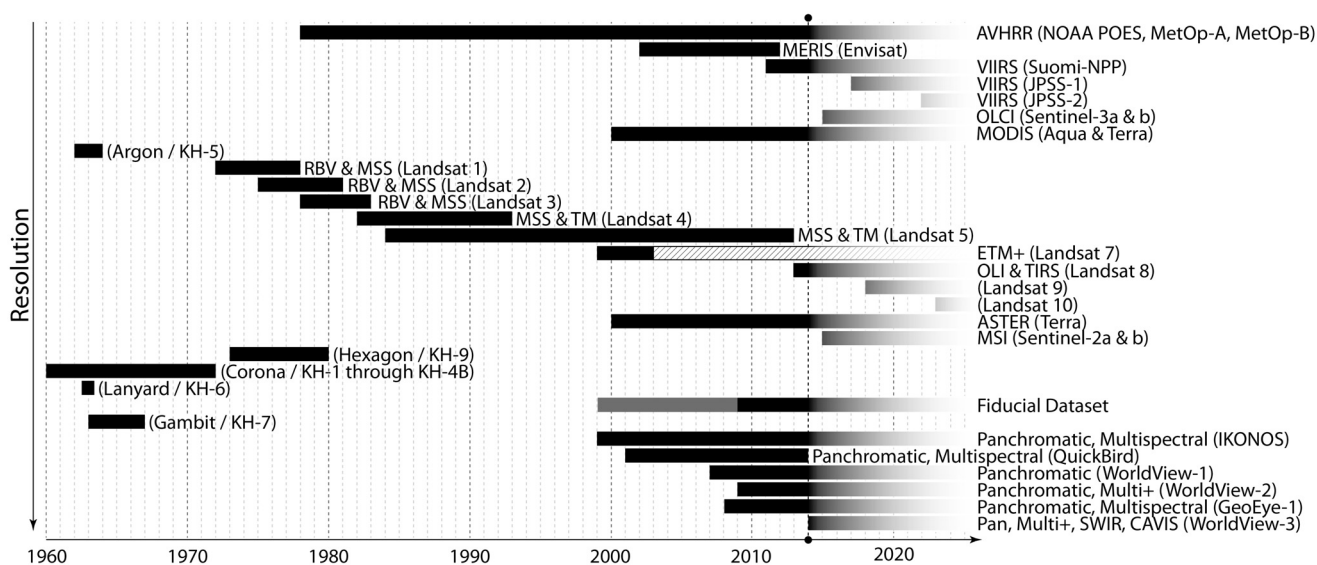
Perhaps the best-known and most widely-used multispectral program, Landsat has been running since 1972, sending back nearly 40 years of continuous Earth observations [2,35]. While originally designed for mapping, land use and natural resources applications, it is not an exaggeration to state that uses of Landsat imagery extend to all areas of polar and cryospheric research. A prime example is the *Satellite Image Atlas of Glaciers of the World* [36]. One of Landsat's greatest strengths is its long history and nearly continuous archive of missions designed to complement and continue each other. In addition, painstaking work has been put into ensuring a radiometrically-consistent dataset across missions [37]. Archival imagery and climate data record are freely available through http://earthexplorer.usgs.gov.

At significantly lower spatial resolution, the perhaps now inaptly named Advanced Very High Resolution Radiometer (AVHRR) was a NOAA multispectral sensor launched in 1978 with a ground resolution of 1.1 km and a swath width of 4000 km. AVHRR sensors have been on many NOAA satellites since and persist to this day. A variety of images and products are available through NOAA's CLASS (http://www.class.ncdc.noaa.gov/), NASA's ECHO REVERB (http://reverb.echo.nasa.gov/) and NSIDC (the National Snow and Ice Data Center, http://nsidc.org/).

AVHRR was improved upon by the MODIS sensors (Moderate-Resolution Imaging Spectroradiometer; 250 m to 1 km pixel size), which derive their scientific value from high temporal resolution and high quality radiometry. MODIS data have, for example, been used to measure daily, seasonal and yearly ice sheet albedo trends [38], to identify melt ponds on Arctic sea ice [39] and to track surface features to measure ice shelf velocities [40]. MODIS data has been stretched, stacked and combined into mosaics of Antarctica (MOA; http://nsidc.org/data/moa/) [41,42] and Greenland (MOG; http://planet.sr.unh.edu/mog/) [43], and data from multiple times provide multiple snapshots of these ice-covered continents and variables, such as grounding lines, coastline, ice edge and more (see Table 2).

Although there are many multispectral imagers that are not listed here, those included in this article are those known to the authors to offer free and open data access.

2.3. Synthetic Aperture Radar

Synthetic Aperture Radar (SAR) is a method of active microwave imaging that uses the echo returns from many radar pulses to create a single image. Because it is an active microwave system, the image shows radar backscatter rather than optical reflectance or emitted radiation; a simplistic way to think of the image is it being related to surface roughness. SAR technology has many research and monitoring applications in the polar regions (e.g., iceberg tracking, glacier and ice sheet velocity measurements, sea ice mapping, lake ice mapping, *etc.*), and especially valuable is the capability to image through cloud cover and during long periods of darkness during polar winters. As such, polar regions have been historically well served by SAR satellites.

There is a history reaching back multiple decades of synthetic aperture radar (SAR) data being collected by the European Space Agency (ESA), as well as subsequent Canadian and Japanese launches (see Figure 2). Early efforts were funded and operated by government funding, directly or indirectly through space agencies. SAR acquisition plans were dictated primarily by science programs, national monitoring requirements and direct commercial/non-commercial requirements. This often led

to patchy and inconsistent coverage. Details are available through data archive search tools, which (as referenced below) are often mission-specific.

Figure 2. Historical, ongoing and future spaceborne SAR missions with some freely available data (based on input from the International Polar Year Space Task Group).
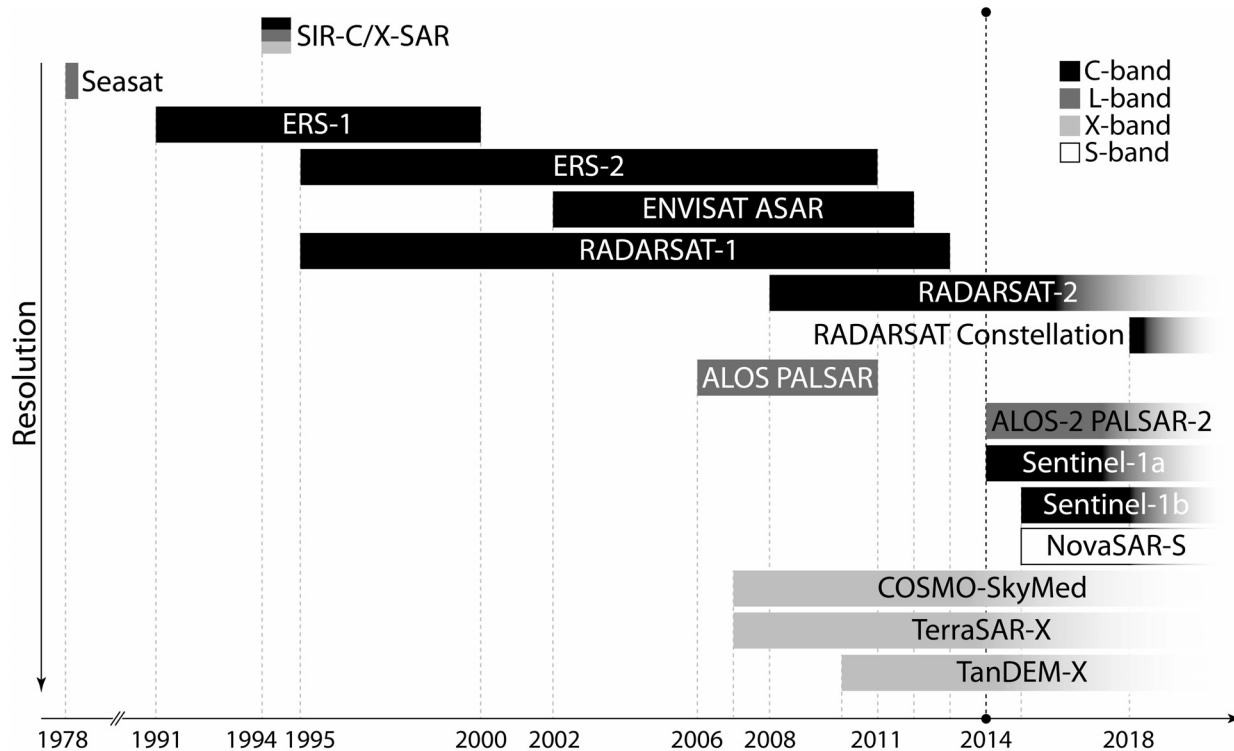
The earliest orbital SAR data ever gathered are from the Seasat mission. Operational for just over 100 days in 1978 before a catastrophic failure, Seasat's SAR collected L-band imagery with 25-m spatial resolution and a ~100-km swath width. Although coverage was limited in spatial extent by available ground stations, Seasat SAR imagery nevertheless has many applications in Arctic North America, Arctic Europe and adjacent seas. Full details and data are available from the Alaska Satellite Facility (https://www.asf.alaska.edu/seasat/) [44].

There has been a historical trend towards an increasing number of SAR imaging modes. Early satellites had only one imaging mode, *i.e.*, fixed extent, resolution and polarization. Historical SAR developments largely focused on the development of C-band sensors. The experimental SIR-C/X-SAR instruments delivered C-, L- and X-band, multipolarization data and was flown on the space shuttle for two missions in 1994; more information on image products is available at (http://edc2.usgs.gov/sir-c/sir-c.php). More recent satellites have a larger number of imaging modes, ranging from wide-area lower resolution modes (used, for example, for operational sea ice monitoring) to smaller-area higher resolution modes (used for targeted acquisitions); these satellites have been in the L-band and, more recently, X-band. Some sensors also have modes focused on interferometric methods, for example for measuring glacier flow velocity and other change detection studies. In addition, there is a parallel trend away from single polarization data, to the collection of dual-polarization and then full quad-polarization data. This has facilitated the development of SAR polarimetry applications.

More recently, SAR satellites have been operated by commercial companies, which will license imagery to pay for the instrument itself, launch and operation. This has led to a perception of high costs for accessing commercial SAR acquisitions, although there are many communities who still have access to these data freely or at low cost (e.g., Alaska Satellite Facility, https://www.asf.alaska.edu/). This is in contrast to fully government-funded and operated satellites, which are moving to free and open data access, like the previously mentioned Landsat program. The trend is increasingly moving in this direction (e.g., European Copernicus Sentinel series, which includes SAR imagers), as there is ongoing difficulty with pricing levels and user uptake for commercial providers.

SAR satellites do not operate a program of regular long-term observations unless they are tasked and paid to do so. All data available are in satellite-specific archives, and the discovery of data frequently relies on requests directly to the commercial satellite operators. There are few tools for online/offline searching of historic archives, and the image search requires communication with satellite customer service desks. For example, ESA's ERS and ENVISAT data can be searched using the EOLI-SA tool (http://earth.esa.int/EOLi/EOLi.html). An easily searchable database for Canadian SAR data back to 1995 was recently made available to the public (https://neodf.nrcan.gc.ca); the SAR images, however, are not freely available. Canadian Arctic RADARSAT-1 data are available at the Canadian Cryospheric Information Network through the Polar Data Catalogue (https://polardata.ca/). More polar-specific resources for access to freely available SAR data are also available via Polar View (http://polarview.aq).

Recent coordination of SAR satellite acquisition and tasking for the polar regions was undertaken during the 2007–2009 International Polar Year through the Space Task Group. This group has now transitioned to be the EC-PORS Polar Space Task Group (Executive Committee-Panel of Experts on Polar Observations, Research and Services), and SAR activities are specifically addressed by its SAR Coordination Working Group (http://www.wmo.int/pages/prog/sat/pstg_en.php).
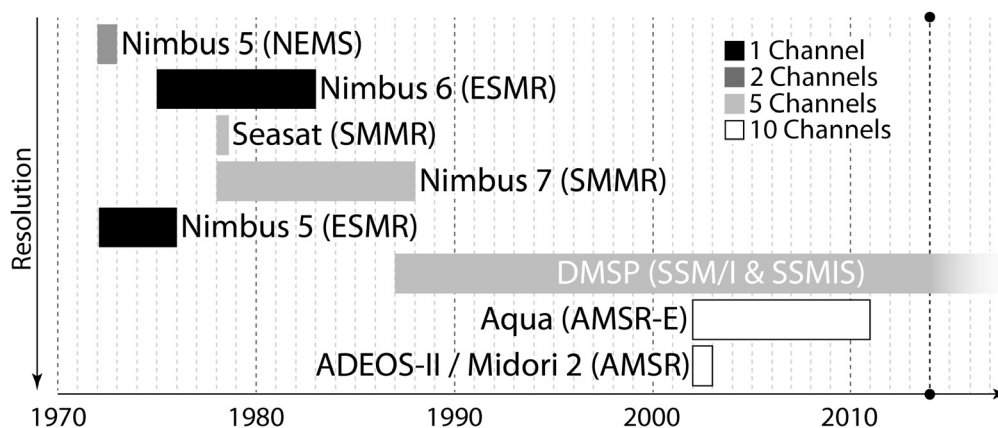
2.4. Passive Microwave

Passive microwave data, as the name implies, involve the detection and measurement of thermal radiation in the microwave region of the electromagnetic spectrum (typically 5–90 GHz) [45]. The fundamental variable that is measured is the brightness temperature. The absorption and emission of radiation by the Earth's atmosphere can be significant, even dominant, in the microwave spectrum, and some instruments are optimized for measuring properties of the atmosphere itself. Others are optimized for measurement of the Earth's surface, and these are the focus of this section.

The brightness temperature [46] is simply the product of the absolute temperature of the emitting material and a dimensionless property called its emissivity, which can take values between zero and one. Most passive microwave radiometers are multispectral instruments, usually with separate channels for different polarization states. These multivariate measurements allow the possibility of deriving a number of different geophysical variables from the data, but note that only some channels are used for surface imaging, while others are used for atmospheric sounding. One of the main applications of passive microwave data is to measure sea and land surface temperatures [47,48]. However, they also have other important applications that are particularly relevant to the cryosphere. These include the measurement of sea ice extent and concentration [49] and various parameters

describing snow cover, both on land [50] and on sea ice [51,52]. A major advantage of passive microwave data is the fact that they can be collected at night and (except at the highest frequencies) through cloud. A major disadvantage is that the spatial resolution of the data (5 km to 50 km) is poor compared with visible-near infrared systems or SAR.

Although terrestrial passive microwave radiometry has been collected from space since the late 1960s (and earlier from Venus, since the Mariner-2 Venus fly-by mission carried a microwave radiometer [53]), the first instruments to provide readily available data that are usefully compatible with those collected today were carried on Nimbus-5, launched in 1972 (see Figure 3). The ESMR (Electrically-Scanned Microwave Radiometer), which collected data from 1972 to 1976, operated at a single frequency of 19.35 GHz, but electrical scanning of the beam gave it an exceptionally wide swath of around 3000 km. The NEMS (Nimbus-E Microwave Spectrometer) was a multichannel instrument, but it viewed only at nadir, with a 185-km footprint, and operated from 1972 to 1973. A longer-lasting ESMR instrument (1975–1983) was carried on-board Nimbus-6, this time operating at 37 GHz (less useful for surface observations). Since 1978, with the launch of Nimbus 7 and the short-lived Seasat, both of which carried the SMMR (Scanning Multichannel Microwave Radiometer) instrument, there has been continuous capability to provide spaceborne multichannel microwave imagery of the Earth's surface. SMMR was a 10-channel instrument, operating at frequencies between 6.6 and 37 GHz and achieving a spatial resolution of around 150 km to 30 km, respectively. Gridded data products, including sea ice properties [54–57] and snow water equivalent [58], are available for the polar regions (and in some cases, the whole world) from NSIDC (http://nsidc.org/data/seaice/pm.html).

Figure 3. Historical and ongoing satellite passive microwave missions (and sensor names) with some freely available data, including the number of surface-imaging channels available for each sensor. NEMS, Nimbus-E Microwave Spectrometer; ESMR, Electrically-Scanned Microwave Radiometer; SMMR, Scanning Multichannel Microwave Radiometer; AMSR-E, Advanced Microwave Sounding Radiometer-Earth Observing System. DMSP, Defense Meteorological Satellite Program; SSM/I, Special Sensor Microwave Imager; SSMIS, Special Sensor Microwave Imager Sounder.

2.5. Active Microwave Scatterometer

Using the same wavelengths as passive microwave and synthetic aperture radar instruments, active scatterometry sends out microwave pulses and measures the returned backscatter at multiple angles. As with other microwave sensors, the returned signal depends on two properties: surface roughness and electrical properties. Originally, scatterometers were designed to measure winds over the open ocean, as derived from surface roughness. However, because scatterometer signals can penetrate some surfaces, they give bulk, as well as surficial information, which is a function of land/sea ice cover. Therefore, they can also be used for land and ice studies, as well.

Scatterometers have relatively low spatial resolution (~25 km to 50 km), but they make up for this with frequent, rapid global coverage in all light and weather conditions. Scatterometers have a range of polar applications. Examples include surface wind field measurements (e.g., [59]), surface melt dynamics (e.g., [60,61]), seasonal melt-freeze transition (e.g., [62]), Greenland ice facies characterization (e.g., [63]) and multi-year sea ice classification (e.g., [64]).

The first satellite scatterometer, SASS (Seasat-A Satellite Scatterometer System), was launched in 1978 aboard the ill-fated Seasat. Since that baseline, further satellites from Europe, the USA, Japan and India have continued the record, including the Advanced Microwave Instrument (AMI) on ERS-1 and ERS-2, the NASA Scatterometer (NSCAT) on ADEOS-I/Midori, SeaWinds on QuikSCAT and ADEOS-II/Midori 2, the Advanced Scatterometer (ASCAT) on MetOp-A and MetOp-B and the Oceansat-2 Scatterometer (OSCAT) on Oceansat-2 (see Figure 4) [65]. Scatterometer sensors vary in the frequency used (C-band or Ku-band), spatial resolution (~25 km to 50 km), antenna azimuth orientations, polarizations, beam resolution, swath width, incidence angle, orbit and coverage. Further scatterometer comparisons are available from NSIDC (http://nsidc.org/data/docs/daac/scatterometer_instrument.gd.html) and the NASA Scatterometer Climate Record Pathfinder (SCP) at Brigham Young University (http://www.scp.byu.edu/data.html).

Figure 4. Historical and ongoing satellite active microwave scatterometer sensors (and platforms) with freely available data, including the frequency band for each sensor. SASS, Seasat-A Satellite Scatterometer System; NSCAT, NASA Scatterometer; ASCAT, Advanced Scatterometer; OSCAT, Oceansat-2 Scatterometer.
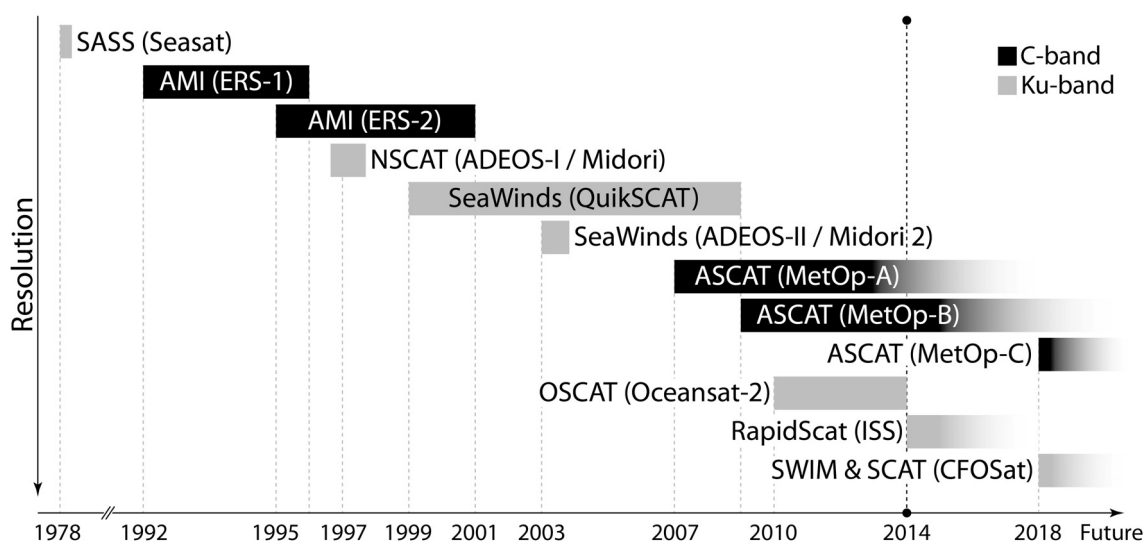
The SCP develops and distributes a variety of scatterometer data products (including backscatter and brightness temperature) and tools designed to support climate studies. SCP typically provides data as enhanced resolution products, improving the ~50 km raw data to a scale of ~2.5 km to 5 km in some cases. The NASA Physical Oceanography Distributed Active Archive Center (PODAAC, http://podaac.jpl.nasa.gov/datasetlist?ids=Measurement&values=Sea Ice) also hosts many overlapping and similar active microwave scatterometer sea ice products. In addition, derived products (e.g., iceberg tracking database, sea ice motion and sea ice age) are included in Section 5 (see Table 2 and http://www.scp.byu.edu/derived.html).

3. Current Data

Increasingly, there are a large variety of data available for polar researchers to see their remote field locations. Indeed, the polar regions are becoming some of the best-mapped areas on the planet. To keep up and take advantage of this, researchers need to know not only what the full arsenal of data is, but how to identify which data are appropriate for their applications and how to get data which is open to them and easily available.

3.1. Multispectral Imagery

As with historical imagery, near-real-time Landsat imagery is freely available, often for immediate download, making it very easy to consult and employ; both quick-looks and full-resolution imagery are available. Of particular interest to polar researchers, large amounts of Landsat data were combined to form the Landsat Image Mosaic of Antarctica (LIMA; lima.usgs.gov) [66]. Landsat 7 with the Enhanced Thematic Mapper Plus (ETM+) onboard was launched in 1999, and while a scan line corrector failed in 2003 [67], it continues to be in operation and used widely. Landsat 8 was launched in February 2013, with operational imagery beginning in April 2013. Landsat 8 adds three additional bands, reduces spectral autocorrelation, improves the signal-to-noise ratio and radiometric resolution (12-bit data) and has other enhancements [68]. In addition, the high-quality georeferencing of Landsat data is of considerable value to users. Landsat 8 acquisitions for the polar regions and cryosphere are an integral part of the long-term acquisition plan.

At lower resolution, the MODIS sensors aboard Terra and Aqua continue to collect imagery. As the MODIS sensors are aging, they have already been joined by the VIIRS sensor (Visible Infrared Imaging Radiometer Suite) on Suomi-NPP. Similar to MODIS, VIIRS imagery has high temporal resolution and low spatial resolution. VIIRS products applicable to the polar regions are still under development, but will be available in the future. Current VIIRS imagery and derivative data records are available through NOAA CLASS (http://www.nsof.class.noaa.gov/).

Landsat, MODIS and VIIRS are NASA instruments, but there are many more multispectral imagers on other nationally- and commercially-run platforms. However, access to these often depends on affiliation or is limited by high cost. For example, affiliation with GLIMS (Global Land Ice Measurements from Space; http://www.glims.org/ [69]) can enable free ASTER imagery, and U.S. federally-funded researchers can access submeter multispectral imagery through the Polar Geospatial Center's (http://www.pgc.umn.edu) RapidIce Viewers (http://www.rapidice.org/viewer). Additionally, it is worthwhile noting that airborne multispectral and hyperspectral imagery is available for

limited coverage areas from the U.K. Natural Environment Research Council (NERC) Airborne Research and Survey Facility (ARSF) via the NERC Earth Observation Data Centre (NEODC; http://www.neodc.rl.ac.uk/). Finally, the IceBridge Digital Mapping System (DMS) provides geolocated and orthorectified high resolution natural color and panchromatic images for many IceBridge flight lines in both the Arctic and the Antarctic (http://nsidc.org/data/iodms1b [70]).

3.2. Synthetic Aperture Radar

Since the loss of ENVISAT in 2012, all currently available SAR satellites are commercially operated. All options (RADARSAT-2 [71], COSMO-SkyMed [72] and TerraSAR-X/TanDEM-X [73]) have a range of imaging modes and capabilities. As was true historically, these satellites do not operate a program of regular long-term observations unless they are tasked and paid to do so. However, since the loss of ENVISAT, the European Commission (EC) and ESA are coordinating current SAR satellites to fill the gap required to support EC-funded Copernicus (formerly GMES) environmental information services. This has resulted in SAR acquisitions over large parts of the Arctic and Antarctic on a regular basis. These data are used for the generation of Copernicus information products, which are freely available online, but the original input SAR data products are not available under the terms of the data license (see http://www.myocean.eu/web/24-catalogue.php). Individual users will likely pay for access to these data if they wish to license their use.

3.3. Passive Microwave

Continuity with SMMR data products has been provided by the operation of the Special Sensor Microwave Imager (SSM/I) carried on the Defense Meteorological Satellite Program (DMSP) series of satellites since 1987. The SSM/I is a seven-channel instrument, operating between 19.35 and 85.5 GHz and achieving a spatial resolution of around 70 km to 16 km, respectively. The SSMIS (Special Sensor Microwave Imager Sounder) instrument has been operated in tandem with the SSM/I since 2005. It has more channels and a frequency range up to 183 GHz, which allows for much more accurate sounding of (and correction for) atmospheric properties. Gridded data products from both of these instruments are available from NSIDC and also include brightness temperature data (http://nsidc.org/data/polar_stereo/data_summaries.html and http://nsidc.org/data/ease/data_summaries.html) [54,57,74–82].

The other principal recent open-access source of passive microwave data from the polar regions is the AMSR-E (Advanced Microwave Sounding Radiometer-Earth Observing System), which was operational from the Aqua satellite between 2002 and 2011. This is a slightly enhanced version of the AMSR that was operational from the ADEOS-II/Midori 2 satellite from 2002 to 2003. AMSR-E is a 12-channel instrument (six frequencies between 6.9 and 89 GHz, each measured in two polarizations), with a spatial resolution of around 56 km to 5.4 km. Gridded data products, accessible from NSIDC at http://nsidc.org/data/amsre/data_summaries/index.html include brightness temperatures, land and sea surface temperatures, sea ice concentration and motion, snow water equivalent and depth, soil moisture, rainfall rate and total monthly precipitation [79,83–89].

Other sources of passive microwave data exist, notably through satellites operated by the European Space Agency. These are generally, at the time of writing (early 2014), not as straightforward to access as the data from the instruments described here.

3.4. Active Microwave Scatterometer

As shown in Figure 4, current scatterometer data are collected only by ESA and EUMETSAT's ASCAT. The C-band ASCAT provides continuity for the AMI sensor aboard ERS-1 and ERS-2. Backscatter image data products are available through the NASA SCP (http://www.scp.byu.edu/data/Ascat/SIR/Ascat_sir.html). In addition, the Indian Space Research Organization and NASA's OSCAT operated from 2010 until February 2014, when it suffered an instrument failure. The Ku-band OSCAT provided continuity for QuickSCAT, although at a slightly different incidence angle. Backscatter image data products are available through the NASA SCP http://www.scp.byu.edu/data/OSCAT/SIR/OSCAT_sir.html). Derived products for both sensors are included in Section 5 (see Table 2 and http://www.scp.byu.edu/derived.html).

4. Future Data

While speculative, this section was compiled with the best available information about upcoming polar and cryospheric missions, as of early 2014.

4.1. Multispectral Imagery

While Landsat 7 is well beyond its planned lifetime, Landsat 8 is young and performing well, and there are two future Landsat missions currently in the planning stages. Although specifications for these missions are still being developed, Landsat 9 is planned for a launch in late 2018, while the launch of Landsat 10 is scheduled for 2023 [2]. As with all current Landsat data, future Landsat missions will provide open and freely available multispectral imagery over almost the entire globe for circumpolar and cryospheric researchers worldwide.

At lower resolutions, VIIRS on-board Suomi-NPP is a bridge mission to NOAA's Joint Polar Satellite System (JPSS). A VIIRS instrument is currently planned to be on-board both JPSS-1, scheduled for launch in early 2017, and JPSS-2, scheduled for launch readiness in early 2022.

The Sentinel satellite series forms the space segment of the EC Copernicus program [90,91]. These satellites are funded by the EC, with ESA responsible for launch and operations. The Sentinel constellation, each version of which is a pair of satellites in itself, will include both higher resolution (10–60 m, Sentinel-2) [92] and lower resolution (300 m, Sentinel-3) [93] multispectral sensors. The first Sentinel-2 and Sentinel-3 are scheduled for launch in 2015. While uncertain until late 2013, in a move away from previous behavior, all Sentinel data will be free and openly available. Registration requirements for data access, however, remain to be seen. Distribution channels are still to be defined, but it is expected that a download manager will be developed along with online FTP access to a rolling archive.

Increasingly, small unmanned airborne systems (UAS's)/unmanned airborne vehicles (UAV's) are capable of collecting high-quality data for local cryospheric mapping needs, both imagery and 3D

point clouds (e.g., [94–96]). Such low-cost and personalized methods for data collection are certainly lowering the barrier to scientists having their own specific datasets, which raises questions not just of data quality, but also documentation and distribution. It remains to be seen if and how researchers will describe and share the data that their drones are collecting.

In addition, constellations of small satellites (e.g., CubeSats) will facilitate higher temporal monitoring from space at spatial resolutions of 1–5 m. Intelligence is still the driver, but they will still have some scientific applications [97]. However, use will be determined not only by data availability and quality, but also by the price of imagery and the distribution of data products, if any.

4.2. Synthetic Aperture Radar

There are advanced plans for continuity of SAR data acquisition covering the polar regions. The lifetimes of current commercial missions extend for a number of years and provide capacity to complement publicly-funded missions. The operators of these commercial platforms also have plans for next generation satellites to extend their capacity into the future. This will likely see the addition of improved capabilities, including higher resolution, larger coverage and more interferometric and polarimetry capabilities.

Four high-profile future publicly-funded missions are currently planned and will have a significant role in providing data for the polar regions. The first satellite in the Sentinel series will be a C-band SAR satellite collecting at a range of spatial resolutions from 5 to 100 m [98]. At the time of writing, Sentinel-1a had been launched on 3 April 2014, sent back its first images on 12 April 2014, and was still in commissioning phase; Sentinel 1-b is scheduled for 2015, both with a seven-year operational lifespan. As with the multispectral Sentinels previously discussed, data are expected to be free and open, with distribution channels still to be defined.

The second mission is JAXA's ALOS-2, which carries the L-band PALSAR-2. Like other SARs, PALSAR-2 has a wide variety of imaging modes in multiple polarizations and with resolutions ranging from 1 m to 100 m. Successfully launched on 24 May 2014, the PALSAR-2 antenna was successfully deployed on 26 May 2014, and has been declared stable (https://directory.eoportal.org/web/eoportal/satellite-missions/a/alos-2). Data quality and availability remain to be seen.

The third publicly funded SAR satellite system is the next phase of the Canadian Radarsat program called the Radarsat Constellation. This is planned for launch in 2018 and comprises three C-band SAR satellites to provide daily monitoring of Canada's land and oceans and the ability to acquire imagery of most of the world's surface. Full mission details are available at http://www.asc-csa.gc.ca/eng/satellites/radarsat/. While it is early in the process and details still need to be determined, initial plans are for this satellite system to be operated by the Canadian Space Agency on a noncommercial basis, which should allow more open access to data.

The fourth mission, still in development, is the U.K.-based NovaSAR-S. With seed funding from the U.K. government, this is another commercial partnership. A constellation of S-band (3.1–3.3 GHz) imagers with a variety of medium-resolution imaging modes (6–30 m) is planned for a 2015 launch, although this is tentative. With an emphasis on low-cost delivery and data priced similar to traditional optical missions, there is some hope that there will be a proportion of the data available for low cost

or free civil and scientific use. However, the scope and delivery methods for such data have not yet been defined.

4.3. Passive Microwave

The future provision of satellite passive microwave imagery of the Earth's surface is not entirely clear. The instruments that have provided much data since the year 2000 have been the AMSR-E on the Aqua satellite and the SSMIS onboard DMSP. AMSR-E failed in 2011, but SSMIS continues to provide data. A DMSP platform with SSMIS successfully was launched in April 2014, and another is planned for launch in 2020.

4.4. Active Microwave Scatterometer

2014 saw the failure of a relatively new scatterometer (OSCAT), but also sees the launch of a new Ku-band scatterometer: RapidScat, mounted on board the International Space Station. RapidScat is currently planned to operate through 2016. The continuity of the C-band scatterometer record appears to be safe with two currently operating ASCATs and the planned 2018 launch of MetOp-C with another ASCAT onboard. A joint Chinese-French platform is also planned for a 2018 launch, carrying two C-band scatterometers: SWIM and SCAT. Further missions are in planning stages and under discussion by groups, such as the Ocean Vector Winds Science Team (http://coaps.fsu.edu/scatterometry/meeting/past.php).

5. Polar Products

Many remote sensing products may be difficult for an inexperienced user to process and interpret. Raw data are processed, projected, resampled or combined to produce derived products for users. Indeed, even for experienced users, a derived product is sometimes more helpful than the raw data. Examples include surface temperature, albedo, sea ice extent, glacier outlines or grounding lines and snow water equivalent/snow depth, vegetation and lithology maps. Based on the provided metadata, it is crucial to understand where products come from, the biases, potential errors and what implications these have for eventual application.

Many of these datasets are easily available, with metadata, through centralized sources, such as the National Snow and Ice Data Center (NSIDC, http://nsidc.org/), Global Cryosphere Watch (http://globalcryospherewatch.org), the World Glacier Monitoring Service (http://www.wgms.ch), the Ocean and Sea Ice Satellite Applications Facility (http://osisaf.met.no/p/ice/) and the Polar Geospatial Center (http://www.pgc.umn.edu/), although others are distributed by individual principal investigators (PIs), or through institutions and consortia, as well. For a list of some polar product providers and notable products themselves, see Table 2. Cryolist, a semi-moderated e-mail distribution list (http://cryolist.org/), also deserves special mention here; this online community of polar and cryospheric researchers can be a helpful resources to find data, to ask questions about tools or methods and to disseminate news about new or updated datasets.

An important set of products is that which uses altimetry data, interferometry or stereo imagery to produce digital elevation models (DEMs). DEMs can be produced utilizing a wide variety of data

types and with varying methodologies, but there are three broad categories: stereo imagery, InSAR (interferometric synthetic aperture radar) and altimeters (both laser and radar).

Stereo pairs of optical imagery were used to produce the 30-m ASTER GDEM and GDEM-2 [99], SPIRIT DEMs from the French SPOT satellites instruments (e.g., [100,101]), some historical DEMs (e.g., [32,33]) and increasingly for stereo WorldView images. With WorldView, the Ames Stereo Pipeline (ASP) is a freely available and popular tool to create DEMs [102,103], although private tools like SETSM [104] and proprietary tools like ERDAS Imagine are also common. A Greenland-specific 30-m DEM created with a combination of stereo imaging and photoclinometry is available at http://bprc.osu.edu/GDG/gimpdem.php [105].

Interferometric synthetic aperture radar was used to produce the 90-m Shuttle Radar Topography Mission (SRTM) DEM (http://www2.jpl.nasa.gov/srtm/; http://www.cgiar-csi.org/data/srtm-90m-digital-elevation-database-v4-1) [106–108], although this DEM does suffer from penetration in low density surfaces (e.g., [109,110]). It is important to note, however, that SRTM does not have polar coverage, being limited to areas between 60°S and 60°N (see http://www2.jpl.nasa.gov/srtm/datacoverage.html). A global DEM based on TerraSAR-X/TanDEM-X data is scheduled for release very soon (12-m spatial resolution, 2-m relative vertical accuracy, 10-m absolute vertical accuracy), although this product is likely to be only commercially available (http://www.astrium-geo.com/worlddem/).

Airborne laser altimetry (e.g., [111–114]), satellite laser altimetry from ICESat (e.g., [115,116]), satellite radar altimetry (e.g., [116,117]), and data fusions, such as photoclinometry [118], have all been employed to produce DEMs. There are a few notable Antarctic DEMs produced, including an improved Antarctic Peninsula 100-m DEM (http://nsidc.org/data/nsidc-0516) [119,120], the RAMP DEM (Radarsat Antarctic Mapping Project, http://nsidc.org/data/nsidc-0082) [121], ICESat ice sheet DEMs (http://nsidc.org/data/docs/daac/nsidc0304_0305_glas_dems.gd.html) for Antarctica (http://nsidc.org/data/nsidc-0304.html) [122] and Greenland (http://nsidc.org/data/nsidc-0305.html) [123] and a DEM produced at the University of Bristol using ERS-1 radar altimetry and ICESat laser altimetry (http://nsidc.org/data/nsidc-0422) [124–126]. For some areas, elevation and other data are available from multiple sensors on NASA's Operation IceBridge via NSIDC (http://nsidc.org/data/icebridge/index.html) [127–129]. In addition, ESA's Cryosat-2 is now producing elevation data at multiple levels for both ice sheet and sea ice studies (http://www.esa.int/Our_Activities/Observing_the_Earth/The_Living_Planet_Programme/Earth_Explorers/CryoSat-2). As an aside, ice-penetrating radar has also been used to produce BEDMAP [130] and Bedmap2 [131], a digital model of the ground beneath Antarctica's ice, as well as a similar map for Greenland [132].

Table 2. Selected open access products derived from polar and cryospheric remote sensing data.

Product Name	Description	URL
Antarctic Digital Database (ADD)	The SCAR (Scientific Committee on Antarctic Research) ADD is a compilation of spatial information for the continent of the Antarctic from 60°S to 90°S. The SCAR ADD consists of geographic information layers, including coastline, ice-shelf grounding line, rock outcrop, elevation data and human presence features, such as research station locations. The ADD is managed for SCAR by the British Antarctic Survey.	http://www.add.scar.org/

Table 2. *Cont.*

Product Name	Description	URL
Antarctic Peninsula DEM	Derived from ASTER GDEM and posted to 100-m spacing, this DEM has been significantly improved for snow and ice covered regions. Using a new smoothing method [119], this DEM achieves a mean elevation difference of −4 ± 25 m when compared to ICESat.	http://nsidc.org/data/nsidc-0516 [120]
Antarctic 1-km DEM from Combined ERS-1 Radar and ICESat Laser Altimetry	This data set provides a 1-km resolution DEM) of Antarctica by combining measurements from the ERS-1 Satellite Radar Altimeter from 1994 and the ICESat Geosciences Laser Altimeter System from 2003 to 2008 [124,125]. Data are provided as two gridded binary files and two ENVI header files viewable using ENVI or other similar software packages.	http://nsidc.org/data/nsidc-0422 [126]
Bedmap2	Bedmap2 is a suite of gridded products describing surface elevation, ice-thickness and the sea floor and subglacial bed elevation of the Antarctic south of 60°S.	http://www.antarctica.ac.uk//bas_research/our_research/az/bedmap2/ [131]
BYU Antarctic Iceberg Database	Using data from six different active microwave scatterometers for 1978 and 1992–present, this database brings together latitude and longitude coordinates for icebergs initially identified by the National Ice Center [133].	http://www.scp.byu.edu/data/iceberg/database1.html
Circumpolar Arctic Vegetation Map (CAVM)	The CAVM defines the spatial extent of dominant vegetation in terms of the dominant plant growth forms and physiognomy. Mapped vegetation extends south to the tree line, which varies with longitude. Spatial coverage is approximately 60°N to 90°N.	http://nsidc.org/data/ggd639 (e.g., [134])
Cryosat-2 Elevation Data	Elevation profiles derived from radar altimetry, in "Level 2" products, as well as more complex raw data. See the ESA website and the appropriate literature for specific applications (*i.e.*, sea ice, ice sheets, *etc.*).	https://earth.esa.int/web/guest/missions/esa-operational-eo-missions/cryosat
Frozen Ground Maps	Various permafrost extent, soil temperature and ground ice maps are available for regions, such as China, Russia, Mongolia, Canada, Alaska and the Circumarctic region.	http://nsidc.org/fgdc/maps/ (e.g., [135])
Glacier Photograph Collection	An online collection of more than 12,000 photographs of glaciers. Largely comprised of images from the Rocky Mountains, the Pacific Northwest, Alaska and Greenland, it also includes select images from Europe and South America. Updates to the dataset are ongoing, and the photos are searchable via a web interface.	https://nsidc.org/data/docs/noaa/g00472_glacier_photos/ [21]
GLAS/ICESat Ice Sheet DEMs	These DEMs of Antarctica (500-m posting) and Greenland (1-km posting) are derived from GLAS/ICESat laser altimetry profile data collected February 2003, to June 2005, providing greater latitudinal extent and fewer slope-related effects than radar altimetry alone. Both DEMs are in polar stereographic grids; the grids cover all of Antarctica north of 86° S and all of Greenland south of 83°N. Elevations for both ice sheets are reported as centimeters above the datums, relative to both the WGS84 Ellipsoid and the EGM96 Geoid. Ancillary files include data quality maps of interpolation distance, as well as ENVI header files.	http://nsidc.org/data/docs/daac/nsidc0304_0305_glas_dems.gd.html; Antarctica: http://nsidc.org/data/nsidc-0304.html [122] and Greenland: http://nsidc.org/data/nsidc-0305.html [123]

Table 2. *Cont.*

Product Name	Description	URL
Global Land Ice Measurements from Space (GLIMS) Glacier Database	The GLIMS project is a large, collaborative endeavor to digitize the world's glaciers using satellite imagery. While the Randolph Glacier Inventory (see below) is a comprehensive snapshot, the GLIMS glacier database offers the ability to study change over time. Provided in multiple vector formats.	http://glims.org/ [69]
GlobICE	The GlobICE project provides measures of sea ice motion, deformation and flux through selected gateways for use in climate modeling and research. Products are derived from radar images taken by ESA's ASAR Wide-Swath on-board ENVISAT and available from 2004 to 2011. The product is available for the Arctic and as a prototype for the Antarctic.	http://www.globice.info
Greenland Bed DEM	A bed elevation dataset for Greenland derived from a combination of multiple airborne ice thickness surveys undertaken between the 1970s and 2012, as well as satellite-derived elevations for non-glaciated terrain to produce a consistent surface over the entire island including across the glaciated-ice-free boundary. The DEM was extended to the continental margin with the aid of bathymetric data. The DEM is interpolated to 1-km postings; errors in bed elevation range from a minimum of ±10 m to about ±300 m, as a function of distance from an observation and local topographic variability.	https://docs.google.com/file/d/0 BylqEEvDu_qtWWdIYTFVcV pkd2s/edit?usp=sharing (NetCDF) and https://docs.google.com/file/d/0 BylqEEvDu_qtWVpsaG1XUk w3eW8/edit?usp=sharing (GeoTIFF) [132]
Greenland Ice Mapping Project (GIMP) DEM and ice mask	The GIMP DEM is constructed from a combination of ASTER and SPOT-5 DEM's for the ice sheet periphery and margin (*i.e.*, below the equilibrium line elevation) south of approximately 82.5°N and AVHRR photoclinometry in the ice sheet interior and far north. The DEM is posted to 30 m, although the "true" resolution of the DEM will vary from 40 m in areas of SPOT-5 coverage to 500 m in areas of photoclinometry. In addition, a raster binary land mask classification for Greenland's ice area is available, mapped from Landsat and RADARSAT imagery. Both the DEM and the ice mask are on the same grid posting, broken into tiles across the continent; ice mask data are also available at 15-m posting.	http://bprc.osu.edu/GDG/gimpd em.php and http://bprc.osu.edu/GDG/icemas k.php [105]
IceBridge	Products derived from aircraft missions using multiple instruments to map ice surface topography [127–129], bedrock topography beneath the ice sheets [136], ice and snow thickness [137] and sea ice distribution and freeboard [138]. Data from laser altimeters and radar sounders are paired with a gravimeter [139,140], magnetometer [141], mapping camera [70] and other data to provide repeat measurements of rapidly-changing portions of land and sea ice.	http://nsidc.org/data/icebridge/
Icelandic Glacier DEMs	Airborne LiDAR DEMs were produced for over 90% of the ice-covered area of Iceland (including Vatnajökull, Hofsjökull, Mýrdalsjoökull, Drangajökull, Eyjafjallajökull and several smaller glaciers) as an International Polar Year deliverable. The DEMs also include a 500 m- to 1 km-wide buffer of proglacial geomorphological features. LiDAR point clouds were averaged and interpolated to produced DEMs gridded at 5-m postings; both the horizontal and vertical accuracy are under 0.5 m [114].	Data are available on request from Tómas Jóhanesson at the Icelandic Meteorological Office (tj@vedur.is). HTTP and FTP download services are in development.

Table 2. *Cont.*

Product Name	Description	URL
Landsat Image Mosaic of Antarctica (LIMA)	Covering the entire Antarctic continent at latitudes lower than 82.5°S, LIMA rigorously combines over 1000 Landsat scenes to visualize the continent in unprecedented quantitative detail [66]. Image mosaics of Antarctica and Greenland using Landsat 8 imagery are in planning stages.	http://lima.usgs.gov/
MODIS Ice Sheet Mosaics	A MODIS Mosaic of Antarctica (MOA, 2003–2004) is available through the NSIDC, imaging the ice sheet, ice shelves and surrounding land area at a grid scale of 125 m and estimated spatial resolution of 150 m. For Greenland, a similar product (MOG, 2005) is available at 100-m grid resolution and an estimated spatial resolution of 100 m to 200 m. MOA includes a corresponding grain size map. There are plans for future MODIS mosaics of both continents.	MOA: https://nsidc.org/data/moa/ [41,42] MOG: http://nsidc.org/data/nsidc-0547 [43]
MODIS Rapid Response Mosaics and the Rapid Ice Sheet Change Observatory (RISCO)	Daily Arctic and Antarctic mosaic images are available in photo-like, true color from both the Terra and Aqua satellites at 4-km, 2-km and 1-km resolutions. The mosaic is composed of smaller image tiles, which are available individually at 250-m, 500-m, 1-km, 2-km and 4-km resolutions. Smaller, cropped areas of interest in the Antarctic are also generated upon request, beginning 4 December 2008, throughout austral late spring, summer and early fall as long as enough visible light is present to generate an image of the region.	http://rapidfire.sci.gsfc.nasa.gov/imagery/subsets/?project=antarctica_regions, …?project=antarctica_risco_areas, …?project=antarctica_usap_ops …?mosaic=Antarctica, and …?mosaic=Arctic
NASA MEaSUREs (Making Earth System data records for Use in Research Environments program)	The MEaSUREs projects function in effect as additional processing facilities for NASA and are subject to rigorous standards, developing consistent global- and continental-scale Earth System Data Records by supporting projects that produce data using proven algorithms and input. Data sets produced include Greenland ice velocity [142–144], Antarctic ice velocity [145–148], Antarctic grounding line position [149,150] and global freeze/thaw maps [151,152].	http://nsidc.org/data/measures/
Polar Geospatial Center DEMs	Stereo DEMs from WorldView imagery are available for areas in Greenland (with coverage soon to expand in both the Arctic and Antarctic) based upon two different processing algorithms (*i.e.*, SETSM [104] and Ames Stereo Pipeline (ASP) [102]). In addition, airborne LiDAR DEMs are available for selected areas in Antarctica's McMurdo Dry Valleys and Ross Island.	http://www.pgc.umn.edu/elevation
QuikSCAT Sea Ice Age	Daily maps of Arctic sea ice age, produced in a standard polar stereographic grid. This product is primarily designed to study multi-year sea ice as opposed to the sea ice edge [64].	http://www.scp.byu.edu/data/Quikscat/iceage/Quikscat_iceage.html
QuikSCAT and SSM/I Merged Sea Ice Motion	Scatterometer and passive microwave sea ice motion vectors complement each other. This data product brings the two together using wavelet techniques [153].	http://www.scp.byu.edu/data/Quikscat/IceMo/Quikscat_icemotion.html
Radarsat Antarctic Mapping Project (RAMP) DEM	Created for (*i.e.*, not by using) Radarsat data processing, this DEM incorporates data from satellite radar altimetry, airborne radar surveys, the Antarctic Digital Database (version 2) and large-scale topographic maps from the USGS and the Australian Antarctic Division. Data were collected between the 1940s and present, with most collected during the 1980s and 1990s. The 1-km, 400-m and 200-m DEM data are provided in ARC/INFO and binary grid formats, and the 1-km and 400-m DEMs are also available in ASCII format.	http://nsidc.org/data/nsidc-0082 [121]

Table 2. *Cont.*

Product Name	Description	URL
Randolph Glacier Inventory (RGI)	Global glacier inventory in vector format. While the RGI is a comprehensive snapshot, the GLIMS glacier database (see above) offers the ability to study change over time.	http://www.glims.org/RGI/randolph.html [154]
Rutgers Global Snow Lab	Northern hemisphere snow cover absolute extent and anomalies at multiple temporal scales. Created using the Interactive Multisensor Snow and Ice Mapping System (http://www.natice.noaa.gov/ims/ims_1.html).	http://climate.rutgers.edu/snowcover/
Scatterometer Ice Extent Products	Sea ice extent products derived from active microwave scatterometer data are available for both NSCAT and QuikSCAT in the Arctic and the Antarctic, provided in the appropriate polar stereographic grids on a near-real-time basis [155].	http://www.scp.byu.edu/data/iceextent.html
Sea Ice Products	A range of both in-depth and very easy-to-use sea ice products are available, including the passive microwave products (e.g., [52,156]), VIR products (e.g., [157,158]), field observations, Multisensor Analyzed Sea Ice Extent (MASIE) [159], Sea Ice Index [160], Sea Ice trends and Climatologies [161], National Ice Center Charts [162] and Northern Hemisphere Ice and Snow Extents [163].	http://nsidc.org/data/seaice/data_summaries.html and http://nsidc.org/data/easytouse.html#seaice
Shuttle Radar Topography Mission (SRTM) DEMs	A DEM gridded at 90-m spatial resolution for all areas on Earth between 60°S and 60°N. In addition to the raw products provided by NASA, some hole-filled versions are available.	http://www2.jpl.nasa.gov/srtm/ and http://www.cgiar-csi.org/data/srtm-90m-digital-elevation-database-v4-1 [106–108]
Soil Moisture	Derived from the Aquarius microwave radiometer, swath and gridded products are available at multiple temporal resolutions ranging from daily to annual.	http://nsidc.org/data/aquarius/index.html [164]
SpecMap Web Viewer	These data, based on WorldView imagery, are spectral indices that highlight compositional variability throughout Antarctica's Central Transantarctic Mountains (83–84°S, 160°W–170°E) [165]. At 5-m spatial resolution, this product has a significantly higher resolution than regional geological maps from the 1960s.	http://www.pgc.umn.edu/about/research/specmap/

6. Earth Observation Tools

All of the data and imagery in the world are useless if one is not able to interpret and interact with them. Downloading the data (see earlier for many links) is just the first step. There are many commercially available, as well as bespoke software packages for handling data (e.g., ERDAS Imagine, ArcGIS, MATLAB, ENVI). However, remote sensing and GIS software is often unwieldy, very expensive and restricted to particular platforms. Increasingly, there are available freeware and open-source tools with extensive and often customizable functionality, although we will try to retain some polar focus for this paper, as this subject is a textbook in itself. Some popular platforms and packages are listed in Table 3. In addition, some researchers have developed specialized packages for all sorts of higher-level analysis, for example geostatistical error estimates [166] or optical feature tracking [167]. As data sharing was discussed in the Introduction, it is worth noting that increasingly, code is becoming recognized as a product of research and is even being included in some definitions of data required to be shared for publication (e.g., [168]). The world of data manipulation is a whole subject on its own, but the visualization and processing of data should never limit a potential user. Just

as the right data are becoming easier to access, so too is remote sensing software an opening field with many solutions for users.

Table 3. Open source and non-commercial tools for polar remote sensing and geographical analysis.

Name	Description	Source
ESA Toolboxes	A set of software packages developed by the European Space Agency specifically to handle data from ESA instruments, as well as a wide range of other remote sensing data.	https://earth.esa.int/web/guest/pi-community/toolboxes
CIAS	CIAS is an image cross-correlation tool built on top of the free IDL Virtual Machine. It can be used for feature tracking of surface displacement, for example to study sea ice movement, permafrost slump, or glacier flow [167]. Another extensively used tool in the glaciology community is COSI-Corr, a plugin within the commercial package ENVI [169].	CIAS: http://www.mn.uio.no/geo/english/research/projects/icemass/cias/ and COSI-Corr: http://www.tectonics.caltech.edu/slip_history/spot_coseis/
GDAL Libraries	A powerful translator library for raster and vector geospatial data formats.	http://www.gdal.org/
Generic Mapping Tools (GMT)	An open source collection of about 80 command-line tools for manipulating geographic and Cartesian data sets.	http://gmt.soest.hawaii.edu/
GNU Octave	A numerical computational language quite similar to MATLAB, so that most programs are easily portable.	http://www.gnu.org/software/octave/
GRASS GIS	Software suite used for geospatial data management and analysis, image processing, graphics and maps production, spatial modeling and visualization.	http://grass.osgeo.org/
ImageJ	Java-based generic raster editor with extensive plugin capabilities.	http://rsb.info.nih.gov/ij/
Multispec	Simple, lightweight geographical/multispectral raster viewer and editor.	https://engineering.purdue.edu/~biehl/MultiSpec/
PROJ.4 Cartographic Projections Library	A library (often implemented in other programs, such as MATLAB, R, QGIS, *etc*.) used for a wide variety of cartographic reprojection.	http://trac.osgeo.org/proj/
Quantum GIS (QGIS)	A free and open source geographical information system to view and edit a range of raster and vector data; programmable with python; integrates with GRASS, GDAL and R.	http://www.qgis.org/
Quantarctica	A collection of Antarctic geographical datasets that works within QGIS.	http://www.quantarctica.org/
R project	A free software environment for statistical computing, data analysis and graphics.	http://www.r-project.org/
SAGA-GIS (System for Automated Geoscientific Analyses)	An open framework for implementing and visualizing a wide variety of spatial algorithms. Running on Windows and Linux, SAGA-GIS integrates well with R, which can be used to execute SAGA commands.	http://www.saga-gis.org/en/index.html

7. Access and Use of Polar Remote Sensing Data

Both the public and the scientific community are interested in polar Earth observation, aesthetically, operationally and intellectually. Indeed, the success of efforts like NASA's Earth Observatory (http://earthobservatory.nasa.gov/) testifies to this curiosity and relevance, as well as the consistently expanding fields of cryospheric and polar science. We have presented information on many (but not an exhaustive list of) sources of open access polar Earth observation, past, present and future. Now, we keep in mind the current widespread attention on the poles, as well as the global importance of polar research, as we consider some of the important trends influencing polar Earth observation science and free, open data access.

Within polar science, and Antarctic science in particular, data sharing has a long legal and traditional basis, with both success stories and ongoing challenges [170]. As mentioned in the sections above, there has been an increasing trend towards free and open data access for remote sensing data products. Data rescue projects, such as scanning and providing free access to over 330,000 aerial photographs by the USGS, is a strong case of Antarctic remote sensing data sharing. Indeed, there are many examples of polar research that could not have happened without free (to researchers) access to remote sensing data, a notable example being Fretwell *et al.*'s synoptic survey of the emperor penguin populations [171], due to the specialized nature of the work and the high commercial cost of the imagery involved. It is worth noting, however, that free access of this imagery is often available only for particular subsets; in the case of WorldView imagery, it is limited to U.S. federally-funded researchers. Landsat data, on the other hand, is available to all and was also crucial to the Fretwell work [172], as well as other studies, for example global glacier mapping (which has benefitted from free ASTER access, as well) [154]. Still, particularly in commercial missions, although the (raw) data themselves are still very expensive, operational or research products (DEMs, for example) can be freely distributed, the decentralized nature of which raises its own issues, such as access to information about processing chains and associated uncertainties.

Nevertheless, the trend in open access remote sensing data was a driving interest behind compiling this paper and indeed seeking to publish it in an open access journal. In many fields, the cost of Earth observation data is hampering scientific progress, for example in biodiversity and tropical forest assessments [173]; in these fields, calls for interagency and inter-platform combinations of imagery are at a roadblock without low-cost or free and open data. Therefore, it is imperative in polar and cryospheric sciences that the research community takes advantage of the open data that are available, proving the value of these data for gaining new knowledge about the poles and the changing cryosphere and how they influence the planet. It is only through showing in practice the true value of free and open remote sensing data and tools that the trend of further data opening will continue to expand.

Particular success stories include the opening of the Landsat archive [2]. However, this success results from many factors, including wide areal coverage of data, the long time period in the Landsat archive, the significant resources dedicated to producing high quality and radiometrically consistent images, the quality of the metadata and the ease of data access. Some of these considerations are discussed below.

Even perceived difficulty in data access is often enough to deter usage, especially when potential alternatives are available. A good case study in data access and use are the MODIS, VIIRS and MERIS

sensors. All are low resolution multispectral imagers, operated by NASA, NOAA and ESA, respectively. However, unlike the other two, MODIS has a wide range of processing levels and products, all of which are searchable and freely downloadable through a variety of platforms. MERIS requires a (simple) application process to ESA, and many VIIRS products are still in development and only available through NOAA, not a traditional source of remote sensing data for many users. It is hardly coincidental that in polar science, MODIS is by far the most widely used of the three, and it strongly suggests that NASA's is the model of data processing and access that other agencies should seek to follow and indeed to improve upon.

Another case study for data access is that of NASA's Operation IceBridge. These airborne missions to study ice masses in the Arctic and Antarctic are meant to bridge between ICESat satellites (ICESat data are available 2003–2009, and ICESat-2 is scheduled for launch in 2017). This means that while surface elevation is a key parameter in IceBridge studies, many other sensors have also been included on the various aircraft, including (but not exhaustively) snow radar, multiple LiDAR instruments, radar altimeters, radio echo sounders, a magnetometer and a gravimeter. All IceBridge data, once they are processed, are available via NSIDC (see Table 2). Although NSIDC's expertise lies in data management and distribution, IceBridge instruments are PI-driven, which means there can be significant differences in data descriptions and a lag time between collection and availability. There is no overarching mechanism and standard processing in place for these data, as there is, for example, behind the Landsat archive. Still, because they are linked spatially, at least IceBridge data are all in one place and searchable in a map interface. This is a good example of diverse types of data being able to be used in a suite.

Taking a step back in time; originally, all remote sensing data were expensive. In the last few decades, the field has seen a huge change. Increasingly, the challenge is no longer just getting any image; it is getting the right image(s) and being able to process them through to a meaningful result, often in an expedient manner. Although there are still restrictions on permitted use and sharing (especially with data from commercial partnerships), the bigger stumbling blocks are often file transfer, processing requirements and access time. The sheer volume of free data available requires expertise from the remote sensing researcher to select the right data and process it with the right steps, whether registration, atmospheric correction, orthorectification or some other necessary step. The cryospheric community is quite rapidly churning out high quality science from large masses of data. Increasingly, it is incumbent upon the remote sensing/cryospheric scientist to also be a *de facto* software engineer in order to do the best science possible, a variable that comes down to both training and collaboration; both important, but not the focus of this paper.

Looking both into the future and historically, a developing trend is not just processing large data sets of recently acquired data; old data enabling new science through data rescue and new ancillary data are increasingly pushing forward our understanding of the poles and the Earth's cryosphere. As discussed in the historical aerial photography section, new calibrations and tie points are allowing researchers to make quantitative use of old images. Data rescue projects are putting old data in useable forms again, for example to extend our knowledge of Arctic and Antarctic sea ice back to 1964 [174]. This latter study shows that the difficulty in pushing back remote sensing time series is often finding the data to begin with.

Therefore, how does one discover and use the best data? It is our hope that this paper provides a starting point and will be sufficient for many. However, the real key to data discovery and use lies in one word: metadata. For the uninitiated, metadata are data about data; in theory, all of the information a user would need to be able to fully utilize the data is provided. For remote sensing data, this can include geographic coverage, type of sensor, date of collection, description of processing level and perhaps what that entails and much, much more. Metadata creates an entire discussion unto itself!

Good metadata increase the life of data (as discussed with historical aerial photography), make data more searchable (especially in the case of diffuse data sets, also mentioned above) and explain the data, such that users apply it properly to their scientific or operational problems. Metadata quality varies hugely and can be all the difference in a researcher's shared output (e.g., a DEM of a particular glacier created from WorldView imagery) being used or not. Large data providers have challenges to face in terms of standardizing across a large portfolio, but metadata are usually significantly more complete from institutions, as compared to individuals.

The rise of the data journal (e.g., *Earth Systems Science Data* or Nature Publishing Group's *Scientific Data*) both encourages and rewards individual PIs to describe and distribute their datasets by giving them citable publications. Indeed, NSIDC is not the only place which can house polar data; the Polar Information Commons (http://www.polarcommons.org/) is a project to "serve as an open, virtual repository for vital scientific data and information and would provide a shared, community-based cyber-infrastructure fostering innovation, improved scientific understanding, and encourage participation in research, education, planning, and management in the polar regions". However, both remote sensing and polar research have their own challenges in data sharing, whether international open data policies, file format or comprehensive description. Through the most recent International Polar Year (2007–2009), the community has begun to identify both success and failures (e.g., [175]), which can be taken forward for polar Earth observation data management and cyberinfrastructure into the future.

8. Conclusions

This paper introduced the main types and sources of remotely sensed data that are freely available and have cryospheric applications, including aerial and satellite photography, satellite-borne visible, near-infrared and thermal infrared sensors, synthetic aperture radar, passive microwave imagers and active microwave scatterometers. Extensive information about these sensors, their cryospheric and polar applications and download sources/timeframes of data availability were provided in text, figures and tables. Derived data products are increasingly available, and examples of such products of particular value in polar and cryospheric research were presented. Information about available free and, where possible, open-source, software tools for reading and processing remotely sensed data were also included.

Into the future, funding for upcoming sensors will continue to be contentious in both the public and private spheres. Support for missions will respond to demonstrated value from sensors, although it will be crucial to push for development missions, too. As we move forward, it is crucial that the community not only utilizes the openly available data, but also continues to tell people about it. Public engagement of many varieties to share beautiful images and compelling success stories is crucial to demonstrate the utility of having free and open access polar remote sensing data; open access

publications by the community will forward this cause, too. Looking ahead, the community (researchers together with data curators and cyberinfrastructure partnerships) will be required to collect, manage and use an increasingly wide variety of polar and cryospheric remote sensing data, the majority of which will likely be trending to even more free and open access. Learning our lessons about the requisite skills, infrastructure, tools and communication of polar Earth observation now will ensure that even better data get into the hands of the researchers that need it; even the ones that do not know it yet.

Acknowledgements

Author Contributions

A. Pope instigated the paper, composed the sections on multispectral remote sensing and active microwave scatterometry, as well as the discussion, created the figures and tables and compiled the contributions of the other authors. W.G. Rees contributed to the sections on passive microwave imagery, shaped significant ideas in the discussion and played a strong role in refining the prose of the paper. A. Fox contributed to the sections on historical aerial photography and to the discussion. A. Fleming contributed to the sections on synthetic aperture radar and to the discussion.

Conflicts of Interest

The authors declare no conflict of interest.

References and Notes

1. Polar Research Board. *Lessons and Legacies of the International Polar Year 2007–2008*; National Academies Press: Washington, DC, USA, 2012.
2. Wulder, M.A.; Masek, J.G.; Cohen, W.B.; Loveland, T.R.; Woodcock, C.E. Opening the archive: How free data has enabled the science and monitoring promise of Landsat. *Remote Sens. Environ.* **2012**, *122*, 2–10, doi:10.1016/j.rse.2012.01.010.
3. Braithwaite, R.J. Glacier mass balance: The first 50 years of international monitoring. *Prog. Phys. Geogr.* **2002**, *26*, 76–95, doi:10.1191/0309133302pp326ra.
4. Sewell, E.D. Distortion—Planigon *versus* metrogon. *Photogramm. Eng. Remote Sens.* **1954**, *20*, 761–764.

5.   Spriggs, R.M. *The Calibration of Military Cartographic Cameras*; U.S. Army Engineer Geodesy, Intelligence and Mapping Research and Development Agency Technical Note; Book on Demand: Wright-Patterson Air Force Base, OH, USA, 1966.

6.   Fox, A.; Cziferszky, A. Unlocking the time capsule of historic aerial photography to measure changes in Antarctic Peninsula glaciers. *Photogramm. Rec.* **2008**, *23*, 51–68, doi:10.1111/j.1477-9730.2008.00463.x.

7.   Kunz, M.; Mills, J.P.; Miller, P.E.; King, M.A.; Fox, A.J.; Marsh, S. Application of surface matching for improved measurements of historic glacier volume change in the Antarctic Peninsula. *Int. Arch. Photogramm. Remote Sens. Spat. Inf. Sci.* **2012**, *XXXIX-B8*, 579–584.

8.   Schenk, T.; Csatho, B.; van der Veen, C.J.; Brecher, H.; Ahn, Y.; Yoon, T. Registering imagery to ICESat data for measuring elevation changes on Byrd Glacier, Antarctica. *Geophys. Res. Lett.* **2005**, *32*, L23S05, doi:10.1029/2005GL024328.

9.   Csatho, B.; Schenk, T.; Van Der Veen, C.J.; Krabill, W.B. Intermittent thinning of Jakobshavn Isbræ, West Greenland, since the Little Ice Age. *J. Glaciol.* **2008**, *54*, 131–144, doi:http://dx.doi.org/10.3189/002214308784409035.

10. Barrand, N.E.; Murray, T.; James, T.D.; Barr, S.L. Optimizing photogrammetric DEMs for glacier volume change assessment using laser-scanning derived ground-control point. *J. Glaciol.* **2009**, *55*, 106–116, doi:http://dx.doi.org/10.3189/002214309788609001.

11. Nuth, C.; Kohler, J.; Aas, H.F.; Brandt, O.; Hagen, J.O. Glacier geometry and elevation changes on Svalbard (1936–1990): A baseline dataset. *Ann. Glaciol.* **2007**, *46*, 106–116, doi:http://dx.doi.org/10.3189/172756407782871440.

12. Nuth, C.; Kohler, J.; König, M.; von Deschwanden, A.; Hagen, J.O.; Kääb, A.; Moholdt, G.; Pettersson, R. Decadal changes from a multi-temporal glacier inventory of Svalbard. *The Cryosphere* **2013**, *7*, 1603–1621, doi:10.5194/tc-7-1603-2013.

13. Tómassen, H. The history of mapping in Iceland, with special reference to glaciers. *Ann. Glaciol.* **1985**, *8*, 4–7.

14. Pálsson, F.; Guðmundsson, S.; Björnsson, H.; Berthier, E.; Magnússon, E.; Guðmundsson, S.; Haraldsson, H.H. Mass and volume changes of Langjökull ice cap, Iceland, 1890 to 2009, deduced from old maps, satellite images and in situ mass balance measurements. *Jökull* **2012**, *62*, 81–95.

15. Bengtsson, T. The mapping of Northern Greenland. *Photogramm. Rec.* **1983**, *11*, 135–150, doi:10.1111/j.1477-9730.1983.tb00466.x.

16. Bjørk, A.A.; Kjær, K.H.; Korsgaard, N.J.; Khan, S.A.; Kjeldsen, K.K.; Andresen, C.S.; Box, J.E.; Larsen, N.K.; Funder, S. An aerial view of 80 years of climate-related glacier fluctuations in southeast Greenland. *Nat. Geosci.* **2012**, *5*, 427–432, doi:10.1038/ngeo1481.

17. LaChapelle, E.R. Assessing glacier mass badgets by reconnaissance aerial photography. *J. Glaciol.* **1962**, *4*, 290–297.

18. Ommanney, C.S.L. The Inventory of Canadian Glaciers: Procedures, Techniques, Progress and Applications. In *World Glacier Inventory*; IAHS: Riederalp, Switzerland, 1980; Volume 126, pp. 35–44.

19. Spencer, R.D.; Hall, R.J. Canadian large-scale aerial photographic systems (LSP). *Photogramm. Eng. Remote Sens.* **1988**, *54*, 475–482.

20. Post, A.; LaChapelle, E.R. *Glacier Ice*; University of Washington Press: Seattle, WA, USA, 2000.

21. NSIDC/WDC for Glaciology, Boulder. *Glacier Photograph Collection*; National Snow and Ice Data Center/World Data Center for Glaciology.: Boulder, CO, USA, 2002; doi:10.7265/N5/NSIDC-GPC-2009-12.

22. Mott, P.G. *Wings over Ice: The Falkland Islands and Dependencies Aerial Survey Expedition*; Peter Mott: Long Sutton, UK, 1986.

23. McHugo, M.B. *Topographical Survey and Mapping of British Antarctic Territory, South Georgia and the South Sandwich Islands 1944–1986*; British Antarctic Survey, Natural Environment Research Council: Cambridge, UK, 2004.

24. *British Antarctic Survey Topographic Map*; Series BAS 250; British Antarctic Survey: Cambridge, UK, 1974.

25. Wrobel, B.P.; Walter, H.; Friehl, M.; Hoppe, U.; Schlüter, M.; Steineck, D. A topographical data set of the Glacier region at San Martin, Marguerite Bay, Antarctic Peninsula. *Polarforschung* **2000**, *67*, 53–63.

26. Rees, W.G. *Remote Sensing of Snow and Ice*; Taylor & Francis: Boca Raton, FL, USA, 2006.

27. Tedesco, M. *Remote Sensing of the Cryosphere*; John Wiley & Sons, Ltd.: New York, NY, USA, 2014.

28. Bindschadler, R. Monitoring ice sheet behavior from space. *Rev. Geophys.* **1998**, *36*, 79–104, doi:10.1029/97RG02669.

29. Dozier, J.; Painter, T.H. Multispectral and hyperspectral remote sensing of alpine snow properties. *Annu. Rev. Earth Planet. Sci.* **2004**, *32*, 465–494, doi:10.1146/annurev.earth.32.101802.120404.

30. Quincey, D.J.; Lucas, R.M.; Richardson, S.D.; Glasser, N.F.; Hambrey, M.J.; Reynolds, J.M. Optical remote sensing techniques in high-mountain environments: Application to glacial hazards. *Prog. Phys. Geogr.* **2005**, *29*, 475–505, doi:10.1191/0309133305pp456ra.

31. König, M.; Winther, J.-G.; Isaksson, E. Measuring snow and glacier ice properties from satellite. *Rev. Geophys.* **2001**, *39*, 1–27, doi:10.1029/1999RG000076.

32. Bolch, T.; Pieczonka, T.; Benn, D.I. Multi-decadal mass loss of glaciers in the Everest area (Nepal Himalaya) derived from stereo imagery. *The Cryosphere* **2011**, *5*, 349–358, doi:10.5194/tc-5-349-2011.

33. Bolch, T.; Buchroithner, M.; Pieczonka, T.; Kunert, A. Planimetric and volumetric glacier changes in the Khumbu Himal, Nepal, since 1962 using Corona, Landsat TM and ASTER data. *J. Glaciol.* **2008**, *54*, 592–600, doi:http://dx.doi.org/10.3189/002214308786570782.

34. Kwok, R. Declassified high-resolution visible imagery for Arctic sea ice investigations: An overview. *Remote Sens. Environ.* **2014**, *142*, 44–56, doi:10.1016/j.rse.2013.11.015.

35. Loveland, T.R.; Dwyer, J.L. Landsat: Building a strong future. *Remote Sens. Environ.* **2012**, *122*, 22–29, doi:10.1016/j.rse.2011.09.022.

36. Williams, R.S.; Ferrigno, J.G. *Satellite Image Atlas of Glaciers of the World*; USGS: Denver, CO, USA, 2013.

37. Markham, B.L.; Helder, D.L. Forty-year calibrated record of earth-reflected radiance from Landsat: A review. *Remote Sens. Environ.* **2012**, *122*, 30–40, doi:10.1016/j.rse.2011.06.026.

38. Box, J.E.; Fettweis, X.; Stroeve, J.C.; Tedesco, M.; Hall, D.K.; Steffen, K. Greenland ice sheet albedo feedback: Thermodynamics and atmospheric drivers. *Cryosphere Discuss.* **2012**, *6*, 593–634, doi:10.5194/tc-6-821-2012.

39. Rösel, A.; Kaleschke, L.; Birnbaum, G. Melt ponds on Arctic sea ice determined from MODIS satellite data using an artificial neural network. *The Cryosphere* **2012**, *6*, 431–446, doi:10.5194/tc-6-431-2012.

40. Haug, T.; Kääb, A.; Skvarca, P. Monitoring ice shelf velocities from repeat MODIS and Landsat data—A method study on the Larsen C ice shelf, Antarctic Peninsula, and 10 other ice shelves around Antarctica. *The Cryosphere* **2010**, *4*, 161–178, doi:10.5194/tc-4-161-2010.

41. Haran, T.; Bohlander, J.; Scambos, T.; Fahnestock, M. *MODIS Mosaic of Antarctica (MOA) Image Map*; National Snow and Ice Data Center: Boulder, CO, USA, 2005; doi:http://dx.doi.org/10.7265/N5ZK5DM5.

42. Scambos, T.A.; Haran, T.M.; Fahnestock, M.A.; Painter, T.H.; Bohlander, J. MODIS-based Mosaic of Antarctica (MOA) data sets: Continent-wide surface morphology and snow grain size. *Remote Sens. Environ.* **2007**, *111*, 242–257, doi:10.1016/j.rse.2006.12.020.

43. Haran, T.; Bohlander, J.; Scambos, T.; Fahnestock, M. *MODIS Mosaic of Greenland (MOG) Image Map*; National Snow and Ice Data Center: Boulder, CO, USA, 2013; doi:http://dx.doi.org/10.7265/N5ZK5DM5.

44. Logan, T.; Holt, B.; Drew, L. The newest oldest data from Seasat's Synthetic Aperture Radar. *Eos Trans. AGU* **2014**, *95*, 93–94, doi:10.1002/2014EO110001.

45. Ulaby, F.T.; Moore, R.K.; Fung, A.K. *Microwave Remote Sensing: Active and Passive. Volume 1—Microwave Remote Sensing Fundamentals and Radiometry*; Artech House: London, UK, 1981.

46. Chang, A.T.C.; Foster, J.L.; Hall, D.K. Nimbus-7 SMMR derived global snow cover parameters. *Ann. Glaciol.* **1987**, *9*, 39–44.

47. Wentz, F.J.; Gentemann, C.; Smith, D.; Chelton, D. Satellite measurements of sea surface temperature through clouds. *Science* **2000**, *288*, 847–850, doi:10.1126/science.288.5467.847.

48. Dash, P.; Göttsche, F.M.; Olesen, F.S.; Fischer, H. Land surface temperature and emissivity estimation from passive sensor data: Theory and practice-current trends. *Int. J. Remote Sens.* **2002**, *23*, 2563–2594.

49. Cavalieri, D.J.; Parkinson, C.L.; Gloersen, P.; Comiso, J.C.; Zwally, H.J. Deriving long-term time series of sea ice cover from satellite passive-microwave multisensor data sets. *J. Geophys. Res.: Oceans* **1999**, *104*, 15803–15814, doi:10.1029/1999JC900081.

50. Goïta, K.; Walker, A.E.; Goodison, B.E. Algorithm development for the estimation of snow water equivalent in the boreal forest using passive microwave data. *Int. J. Remote Sens.* **2003**, *24*, 1097–1102.

51. Gloersen, P.; Campbell, W.J.; Cavalieri, D.J.; Comiso, J.C.; Parkinson, C.L.; Zwally, H.J. *Arctic and Antarctic Sea Ice, 1978–1987: Satellite Passive-Microwave Observations and Analysis*; NASA: Washington, DC, USA, 1992.

52. Anderson, M.; Bliss, A. C.; Tschudi, M. *MEaSUREs Arctic Sea Ice Characterization Daily 25 km EASE-Grid 2.0*; NASA DAAC National Snow and Ice Data Center: Boulder, CO, USA, 2014; doi:http://dx.doi.org/10.5067/MEASURES/CRYOSPHERE/nsidc-0532.001.

53. Njoku, E.G. Passive microwave remote sensing of the earth from space #8212; A review. *Proc. IEEE* **1982**, *70*, 728–750.

54. Cavalieri, D.J.; Parkinson, C.L.; Gloerson, P.; Zwally, H.J. *Sea Ice Concentrations from Nimbus-7 SMMR and DMSP SSM/I-SSMIS Passive Microwave Data*; NASA DAAC National Snow and Ice Data Center: Boulder, CO, USA, 1996.

55. Parkinson, C.L.; Comiso, J.C.; Zwally, H.J. *Nimbus-5 ESMR Polar Gridded Brightness Temperatures. Version 2*; NASA DAAC National Snow and Ice Data Center: Boulder, CO, USA, 1999.

56. Gloerson, P. *Nimbus-7 SMMR Polar Gridded Radiances and Sea Ice Concentrations*; NASA DAAC National Snow and Ice Data Center: Boulder, CO, USA, 2006.

57. Comiso, J.C. *Bootstrap Sea Ice Concentrations from Nimbus-7 SMMR and DMSP SSM/I-SSMIS, Version 2*; NASA DAAC National Snow and Ice Data Center: Boulder, CO, USA, 2014.

58. Armstrong, R.; Brodzik, M.J.; Knowles, K.; Savoie, M. *Global Monthly EASE-Grid Snow Water Equivalent Climatology*; NASA DAAC National Snow and Ice Data Center: Boulder, CO, USA, 2005.

59. Draper, D.W.; Long, D.G. An assessment of SeaWinds on QuikSCAT wind retrieval. *J. Geophys. Res. Oceans* **2002**, *107*, 3212, doi:10.1029/2002JC001330.

60. Trusel, L.D.; Frey, K.E.; Das, S.B. Antarctic surface melting dynamics: Enhanced perspectives from radar scatterometer data. *J. Geophys. Res.* **2012**, *117*, F02023, doi:10.1029/2011JF002126.

61. Ashcraft, I.S.; Long, D.G. Differentiation between melt and freeze stages of the melt cycle using SSM/I channel ratios. *IEEE Trans. Geosci. Remote Sens.* **2005**, *43*, 1317–1323, doi:10.1109/TGRS.2005.845642.

62. Mortin, J.; Howell, S.E.L.; Wang, L.; Derksen, C.; Svensson, G.; Graversen, R.G.; Schrøder, T.M. Extending the QuikSCAT record of seasonal melt–freeze transitions over Arctic sea ice using ASCAT. *Remote Sens. Environ.* **2014**, *141*, 214–230, doi:10.1016/j.rse.2013.11.004.

63. Ashcraft, I.S.; Long, D.G. Observation and characterization of radar backscatter over Greenland. *IEEE Trans. Geosci. Remote Sens.* **2005**, *43*, 225–237, doi:10.1109/TGRS.2004.841484.

64. Swan, A.M.; Long, D.G. Multiyear Arctic sea ice classification using QuikSCAT. *IEEE Trans. Geosci. Remote Sens.* **2012**, *50*, 3317–3326, .

65. Long, D.G.; Drinkwater, M.R.; Holt, B.; Saatchi, S.; Bertoia, C. Global ice and land climate studies using scatterometer image data. *Eos Trans. AGU* **2001**, *82*, 503–503, doi:10.1029/01EO00303.

66. Bindschadler, R.; Vornberger, P.; Fleming, A.; Fox, A.; Mullins, J.; Binnie, D.; Paulsen, S.J.; Granneman, B.; Gorodetzky, D. The Landsat image mosaic of Antarctica. *Remote Sens. Environ.* **2008**, *112*, 4214–4226, doi:10.1016/j.rse.2008.07.006.

67. *NASA Landsat 7 Science Data Users Handbook*; NASA Goddard Space Flight Center: Greenbelt, MD, USA, 2011.

68. Roy, D.P.; Wulder, M.A.; Loveland, T.R.; Woodcock, C.E.; Allen, R.G.; Anderson, M.C.; Helder, D.; Irons, J.R.; Johnson, D.M.; Kennedy, R.; *et al*. Landsat-8: Science and product vision for terrestrial global change research. *Remote Sens. Environ.* **2014**, *145*, 154–172, doi:10.1016/j.rse.2014.02.001.

69. GLIMS. *GLIMS Glacier Database*; National Snow and Ice Data Center: Boulder, CO, USA, 2005; doi:http://dx.doi.org/10.7265/N5V98602.

70. Dominguez, R. *IceBridge DMS L1B Geolocated and Orthorectified Images*; NASA DAAC National Snow and Ice Data Center: Boulder, CO, USA, 2010.

71. Morena, L.C.; James, K.V.; Beck, J. An introduction to the RADARSAT-2 mission. *Can. J. Remote Sens.* **2004**, *30*, 221–234, doi:10.5589/m04-004.

72. Coletta, A.; Angino, G.; Battazza, F.; Caltagirone, F.; Impagnatiello, F.; Valentini, G.; Capuzi, A.; Fagioli, S.; Leonardi, R. *COSMO-SkyMed Program: Utilization and Description of an Advanced Space EO Duel-Use Asset*; IAF: Montreux, Switzerland, 2007.

73. Krieger, G.; Moreira, A.; Fiedler, H.; Hajnsek, I.; Werner, M.; Younis, M.; Zink, M. TanDEM-X: A satellite formation for high-resolution SAR interferometry. *IEEE Trans. Geosci. Remote Sens.* **2007**, *45*, 3317–3341.

74. Anderson, M.; Bliss, A.; Drobot, S. *Snow Melt Onset Over Arctic Sea Ice from SMMR and SSM/I-SSMIS Brightness Temperatures. Version 3*; NASA DAAC National Snow and Ice Data Center: Boulder, CO, USA, 2014.

75. Armstrong, R.; Knowles, K.; Brodzik, M.J.; Hardman, M.A. *DMSP SSM/I-SSMIS Pathfinder Daily EASE-Grid Brightness Temperatures. Version 2*; NASA DAAC National Snow and Ice Data Center: Boulder, CO, USA, 1994.

76. Brodzik, M.J.; Armstrong, R.; Savoie, M. *Global EASE-Grid 8-Day Blended SSM/I and MODIS Snow Cover*; NASA DAAC National Snow and Ice Data Center: Boulder, CO, USA, 2007.

77. Brodzik, M.J.; Armstrong, R. *Near-Real-Time DMSP SSM/I-SSMIS Pathfinder Daily EASE-Grid Brightness Temperatures*; NASA DAAC National Snow and Ice Data Center: Boulder, CO, USA, 2008.

78. Cavalieri, D.J.; Gloerson, P.; Zwally, H.J. *Near-Real-Time DMSP SSM/I-SSMIS Daily Polar Gridded Brightness Temperatures*; NASA DAAC National Snow and Ice Data Center: Boulder, CO, USA, 1999.

79. Long, D.G.; Stroeve, J. *Enhanced-Resolution SSM/I and AMSR-E Daily Polar Brightness Temperatures*; NASA DAAC National Snow and Ice Data Center: Boulder, CO, USA, 2011.

80. Maslanik, J.; Stroeve, J.C. *Near-Real-Time DMSP SSM/I-SSMIS Daily Polar Gridded Sea Ice Concentrations*; NASA DAAC National Snow and Ice Data Center: Boulder, CO, USA, 1999.

81. Maslanik, J.; Stroeve, J. *DMSP SSM/I-SSMIS Daily Polar Gridded Brightness Temperatures. Version 4*; NASA DAAC National Snow and Ice Data Center: Boulder, CO, USA, 2004.

82. Nolin, A.; Armstrong, R.; Maslanik, J. *Near-Real-Time SSM/I-SSMIS EASE-Grid Daily Global Ice Concentration and Snow Extent. Version 4*; NASA DAAC National Snow and Ice Data Center: Boulder, CO, USA, 1998.

83. Cavalieri, D.J.; Markus, T.; Comiso, J.C. *AMSR-E/Aqua Daily L3 12.5 km Brightness Temperature, Sea Ice Concentration, & Snow Depth Polar Grids. Version 2*; NASA DAAC National Snow and Ice Data Center: Boulder, CO, USA, 2003; doi:http://dx.doi.org/10.5067/AMSR-E/AE_SI12.002.

84. Cavalieri, D.J.; Markus, T.; Comiso, J.C. *AMSR-E/Aqua Daily L3 6.25 km 89 GHz Brightness Temperature Polar Grids. Version 2*; NASA DAAC National Snow and Ice Data Center: Boulder, CO, USA, 2004; doi:http://dx.doi.org/10.5067/AMSR-E/AE_SI6.002.

85. Cavalieri, D.J.; Markus, T.; Comiso, J.C. *AMSR-E/Aqua Daily L3 25 km Brightness Temperature & Sea Ice Concentration Polar Grids. Version 2*; NASA DAAC National Snow and Ice Data Center: Boulder, CO, USA, 2004; doi:http://dx.doi.org/10.5067/AMSR-E/AE_SI25.002.

86. Knowles, K.; Savoie, M.; Armstrong, R.; Brodzik, M.J. *AMSR-E/Aqua Daily EASE-Grid Brightness Temperatures*; NASA DAAC National Snow and Ice Data Center: Boulder, CO, USA, 2006.

87. Tedesco, M.; Kelly, R.; Foster, J.L.; Chang, A.T.C. *AMSR-E/Aqua Daily L3 Global Snow Water Equivalent EASE-Grids. Version 2*; NASA DAAC National Snow and Ice Data Center: Boulder, CO, USA, 2004; doi:http://dx.doi.org/10.5067/AMSR-E/AE_DYSNO.002.

88. Tedesco, M.; Kelly, R.; Foster, J.L.; Chang, A.T.C. *AMSR-E/Aqua 5-Day L3 Global Snow Water Equivalent EASE-Grids, Verson 2*; NASA DAAC National Snow and Ice Data Center: Boulder, CO, USA, 2004; doi:http://dx.doi.org/10.5067/AMSR-E/AE_5DSNO.002.

89. Tedesco, M.; Kelly, R.; Foster, J.L.; Chang, A.T.C. *AMSR-E/Aqua Monthly L3 Global Snow Water Equivalent EASE-Grids. Version 2*; NASA DAAC National Snow and Ice Data Center: Boulder, CO, USA, 2004; doi:http://dx.doi.org/10.5067/AMSR-E/AE_MOSNO.002.

90. Berger, M.; Moreno, J.; Johannessen, J.A.; Levelt, P.F.; Hanssen, R.F. ESA's sentinel missions in support of Earth system science. *Remote Sens. Environ.* **2012**, *120*, 84–90, doi:10.1016/j.rse.2011.07.023.

91. Malenovský, Z.; Rott, H.; Cihlar, J.; Schaepman, M.E.; García-Santos, G.; Fernandes, R.; Berger, M. Sentinels for science: Potential of Sentinel-1, -2, and -3 missions for scientific observations of ocean, cryosphere, and land. *Remote Sens. Environ.* **2012**, *120*, 91–101, doi:10.1016/j.rse.2011.09.026.

92. Drusch, M.; Del Bello, U.; Carlier, S.; Colin, O.; Fernandez, V.; Gascon, F.; Hoersch, B.; Isola, C.; Laberinti, P.; Martimort, P.; *et al*. Sentinel-2: ESA's optical high-resolution mission for GMES operational services. *Remote Sens. Environ.* **2012**, *120*, 25–36, doi:10.1016/j.rse.2011.11.026.

93. Donlon, C.; Berruti, B.; Buongiorno, A.; Ferreira, M.-H.; Féménias, P.; Frerick, J.; Goryl, P.; Klein, U.; Laur, H.; Mavrocordatos, C.; *et al*. The Global Monitoring for Environment and Security (GMES) Sentinel-3 mission. *Remote Sens. Environ.* **2012**, *120*, 37–57, doi: 10.1016/j.rse.2011.07.024.

94. Whitehead, K.; Moorman, B.J.; Hugenholtz, C.H. Brief communication: Low-cost, on-demand aerial photogrammetry for glaciological measurement. *The Cryosphere* **2013**, *7*, 1879–1884.

95. Lucieer, A.; Turner, D.; King, D.H.; Robinson, S.A. Using an Unmanned Aerial Vehicle (UAV) to capture micro-topography of Antarctic moss beds. *Int. J. Appl. Earth Obs. Geoinf.* **2014**, *27*, 53–62.

96. Immerzeel, W.W.; Kraaijenbrink, P.D.A.; Shea, J.M.; Shrestha, A.B.; Pellicciotti, F.; Bierkens, M.F.P.; de Jong, S.M. High-resolution monitoring of Himalayan glacier dynamics using unmanned aerial vehicles. *Remote Sens. Environ.* **2014**, *150*, 93–103.

97. Butler, D. Many eyes on Earth. *Nature* **2014**, *505*, 143–144.

98. Torres, R.; Snoeij, P.; Geudtner, D.; Bibby, D.; Davidson, M.; Attema, E.; Potin, P.; Rommen, B.; Floury, N.; Brown, M.; *et al*. GMES Sentinel-1 mission. *Remote Sens. Environ.* **2012**, *120*, 9–24.

99. Tachikawa, T.; Kaku, M.; Iwasaki, A.; Gesch, D.; Oimoen, M.; Zhang, Z.; Danielson, J.; Krieger, T.; Curtis, B.; Haase, J.; *et al*. *ASTER Global Digital Elevation Model Version 2—Summary of Validation Results*; NASA Land Processes DAAC: Sioux Falls, SD, USA, 2011.

100. Korona, J.; Berthier, E.; Bernard, M.; Rémy, F.; Thouvenot, E. SPIRIT. SPOT 5 stereoscopic survey of Polar Ice: Reference Images and Topographies during the fourth International Polar Year (2007–2009). *ISPRS J. Photogramm. Remote Sens.* **2009**, *64*, 204–212, doi:10.1016/j.isprsjprs.2008.10.005.

101. Berthier, E.; Björnsson, H.; Pálsson, F.; Feigl, K.L.; Llubes, M.; Rémy, F. The level of the Grímsvötn subglacial lake, Vatnajökull, Iceland, monitored with SPOT5 images. *Earth Planet. Sci. Lett.* **2006**, *243*, 293–302.

102. Moratto, Z.M.; Broxton, M.J.; Beyer, R.A.; Lundy, M.; Husmann, K. Ames Stereo Pipeline, NASA's Open Source Automated Stereogrammetry Software. In Proceedings of the 41st Lunar and Planetary Science Conference, Woodlands, TX, USA, 1–5 March 2010; Volume 41, p. 2364.

103. Shean, D.E.; Joughin, I.; Smith, B.; Moratto, Z.M.; Porter, C.; Morin, P. Quantifying Ice-Sheet/Ice-Shelf Dynamics and Variability with Meter-Scale DEM and Velocity Timeseries. In Proceedings of 2012 American Geophysical Union Fall Meeting, San Francisco, CA, USA, 3–7 December 2012.

104. Noh, M.-J.; Howat, I. Surface Extraction with TIN-Based Search-Space Minimization (SETSM): Fully Automatic Stereo-Photogrammetric Digital Elevation Model (DEM) Extraction from Pushbroom Satellite Imagery; 1 October 2013. Available online: http://www.pgc.umn.edu/system/files/SETSM_Product_Sheet_v1.1.pdf (accessed on 26 June 2014).

105. Howat, I.M.; Negrete, A.; Smith, B.E. The Greenland Ice Mapping Project (GIMP) land classification and surface elevation datasets. *Cryosphere Discuss.* **2014**, *8*, 453–478.

106. Bernhard Rabus, M.E. The shuttle radar topography mission—A new class of digital elevation models acquired by spaceborne radar. *ISPRS J. Photogramm. Remote Sens.* **2003**, *57*, 241–262, doi:10.1016/S0924-2716(02)00124-7.

107. Farr, T.G.; Rosen, P.A.; Caro, E.; Crippen, R.; Duren, R.; Hensley, S.; Kobrick, M.; Paller, M.; Rodriguez, E.; Roth, L.; *et al*. The Shuttle Radar Topography Mission. *Rev. Geophys.* **2007**, *45*, RG2004, doi:10.1029/2005RG000183.

108. Jarivs, A.; Reuter, H.I.; Nelson, A.; Guevara, E. Hole-Filled SRTM for the Globe Version 4. In *CGIAR-CSI SRTM 90 m Database*; 2008. Available online: http://srtm.csi.cgiar.org (accessed on 5 June 2014).

109. Rignot, E.; Echelmeyer, K.; Krabill, W. Penetration depth of interferometric synthetic-aperture radar signals in snow and ice. *Geophys. Res. Lett.* **2001**, *28*, 3501–3504, doi:10.1029/2000GL012484.

110. Gardelle, J.; Berthier, E.; Arnaud, Y. Impact of resolution and radar penetration on glacier elevation changes computed from DEM differencing. *J. Glaciol.* **2012**, *58*, 419–422.

111. Arendt, A.A.; Echelmeyer, K.A.; Harrison, W.D.; Lingle, C.S.; Valentine, V.B. Rapid wastage of Alaska glaciers and their contribution to rising sea level. *Science* **2002**, *297*, 382–386, doi:10.1126/science.1072497.

112. Rees, W.G.; Arnold, N.S. Mass balance and dynamics of a valley glacier measured by high-resolution LiDAR. *Polar Rec.* **2007**, *43*, 311–319, doi:http://dx.doi.org/10.1017/S0032247407006419.

113. Barrand, N.E.; James, T.D.; Murray, T. Spatio-temporal variability in elevation changes of two high-Arctic valley glaciers. *J. Glaciol.* **2010**, *56*, 771.

114. Jóhannesson, T.; Björnsson, H.; Magnússon, E.; Guðmundsson, S.; Pálsson, F.; Sigurðsson, O.; Thorsteinsson, T.; Berthier, E. Ice-volume changes, bias estimation of mass-balance measurements and changes in subglacial lakes derived by lidar mapping of the surface of Icelandic glaciers. *Ann. Glaciol.* **2013**, *54*, 63–74.

115. Abdalati, W.; Zwally, H.J.; Bindschadler, R.A.; Csathó, B.; Farrell, S.L.; Fricker, H.A.; Harding, D.; Kwok, R.; Lefsky, M.; Markus, T.; *et al*. The ICESat-2 Laser Altimetry mission. *Proc. IEEE* **2010**, *98*, 735–751.

116. Pritchard, H.D.; Luthcke, S.B.; Fleming, A.H. Understanding ice-sheet mass balance: Progress in satellite altimetry and gravimetry. *J. Glaciol.* **2010**, *56*, 1151–1161.

117. Fricker, H.A.; Padman, L. Thirty years of elevation change on Antarctic Peninsula ice shelves from multi-mission satellite radar altimetry. *J. Geophys. Res.* **2012**, doi:10.1029/2011JC007126.

118. Pope, A.; Willis, I.C.; Rees, W.G.; Arnold, N.S.; Pálsson, F. Combining airborne lidar and Landsat ETM+ data with photoclinometry to produce a digital elevation model for Langjökull, Iceland. *Int. J. Remote Sens.* **2013**, *34*, 1005–1025.

119. Cook, A.J.; Murray, T.; Luckman, A.; Vaughan, D.G.; Barrand, N.E. A new 100-m Digital Elevation Model of the Antarctic Peninsula derived from ASTER Global DEM: Methods and accuracy assessment. *Earth Syst. Sci. Data* **2012**, *4*, 129–142.

120. Cook, A.J.; Murray, T.; Luckman, A.; Vaughan, D.G.; Barrand, N.E. *Antarctic Peninsula 100 m Digital Elevation Model Derived from ASTER GDEM*; National Snow and Ice Data Center: Boulder, CO, USA, 2012; doi:http://dx.doi.org/10.7265/N58K7711.

121. Liu, H.; Jezek, K.; Li, B.; Zhao, Z. *Radarsat Antarctic Mapping Project Digital Elevation Model Version 2*; National Snow and Ice Data Center: Boulder, CO, USA, 2001.

122. DiMarzio, J.; Brenner, A.; Schutz, R.; Shuman, C.A.; Zwally, H.J. *GLAS/ICESat 500 m Laser Altimetry Digital Elevation Model of Antarctica*; National Snow and Ice Data Center: Boulder, CO, USA, 2007.

123. DiMarzio, J.; Brenner, A.; Schutz, R.; Shuman, C.A.; Zwally, H.J. *GLAS/ICESat 1 km Laser Altimetry Digital Elevation Model of Greenland*; National Snow and Ice Data Center: Boulder, CO, USA, 2007.

124. Bamber, J.L.; Gomez-Dans, J.L.; Griggs, J.A. A new 1 km digital elevation model of the Antarctic derived from combined satellite radar and laser data—Part 1: Data and methods. *The Cryosphere* **2009**, *3*, 101–111.

125. Griggs, J.A.; Bamber, J.L. A new 1 km digital elevation model of Antarctica derived from combined radar and laser data—Part 2: Validation and error estimates. *The Cryosphere* **2009**, *3*, 113–123.

126. Bamber, J.L.; Gomez-Dans, J.L.; Griggs, J.A. *Antarctic 1 km Digital Elevation Model (DEM) from Combined ERS-1 Radar and ICESat Laser Satellite Altimetry*; National Snow and Ice Data Center: Boulder, CO, USA, 2009.

127. Blair, J.B.; Hofton, M.A. *IceBridge LVIS L2 Geolocated Surface Elevation Product*; NASA DAAC National Snow and Ice Data Center: Boulder, CO, USA, 2012.

128. Larsen, C.F. *IceBridge UAF Lidar Scanner L1B Geolocated Surface Elevation Triplets*; NASA DAAC National Snow and Ice Data Center: Boulder, CO, USA, 2013.

129. Krabill, W. *IceBridge ATM L2 Icessn Elevation, Slope, and Roughness. Version 2*; NASA DAAC National Snow and Ice Data Center: Boulder, CO, USA, 2014.

130. Lythe, M.B.; Vaughan, D.G. BEDMAP: A new ice thickness and subglacial topographic model of Antarctica. *J. Geophys. Res.* **2001**, *106*, 351.

131. Fretwell, P.; Pritchard, H.D.; Vaughan, D.G.; Bamber, J.L.; Barrand, N.E.; Bell, R.; Bianchi, C.; Bingham, R.G.; Blankenship, D.D.; Casassa, G.; *et al.* Bedmap2: Improved ice bed, surface and thickness datasets for Antarctica. *The Cryosphere* **2013**, *7*, 375–393.

132. Bamber, J.L.; Griggs, J.A.; Hurkmans, R.T.W.L.; Dowdeswell, J.A.; Gogineni, S.P.; Howat, I.; Mouginot, J.; Paden, J.; Palmer, S.; Rignot, E.; *et al.* A new bed elevation dataset for Greenland. *The Cryosphere* **2013**, *7*, 499–510.

133. Stuart, K.M.; Long, D.G. Tracking large tabular icebergs using the SeaWinds Ku-band microwave scatterometer. *Deep Sea Res. Part II Top. Stud. Ocean.* **2011**, *58*, 1285–1300, doi:10.1016/j.dsr2.2010.11.004.

134. Walker, D.A. An integrated vegetation mapping approach for northern Alaska (1:4 M scale). *Int. J. Remote Sens.* **1999**, *20*, 2895–2920.

135. Brown, J.; Ferrians, O.; Heginbottom, J.A.; Melnikov, E. *Circum-Arctic Map of Permafrost and Ground-Ice Conditions*; National Snow and Ice Data Center: Boulder, CO, USA, 2014.

136. Allen, C. *IceBridge MCoRDS L3 Gridded Ice Thickness, Surface, and Bottom, Version 2*; NASA DAAC National Snow and Ice Data Center: Boulder, CO, USA, 2014.

137. Leuschen, C. *IceBridge Snow Radar L1B Geolocated Radar Echo Strength Profiles*; NASA DAAC National Snow and Ice Data Center: Boulder, CO, USA, 2013.

138. Kurtz, N.; Studinger, M.; Harbeck, J.P.; Onana, V.D.; Farrell, S. *IceBridge Sea Ice Freeboard, Snow Depth, and Thickness*; NASA DAAC National Snow and Ice Data Center: Boulder, CO, USA, 2014.

139. Cochran, J.R.; Bell, R.E. *IceBridge Sander AIRGrav L1B Geolocated Free Air Gravity Anomalies*; NASA DAAC National Snow and Ice Data Center: Boulder, CO, USA, 2013.

140. Tinto, K.J.; Bell, R.E. *IceBridge Sander AIRGrav L3 Bathymetry*; NASA DAAC National Snow and Ice Data Center: Boulder, CO, USA, 2011.

141. Cochran, J.R.; Burton, B.; Frearson, N.; Tinto, K.J. *IceBridge Scintrex CS-3 Cesium Magnetometer L1B Geolocated Magnetic Anomalies*; NASA DAAC National Snow and Ice Data Center: Boulder, CO, USA, 2012.

142. Joughin, I.; Smith, B.; Howat, I.; Scambos, T.; Moon, T. Greenland flow variability from ice-sheet-wide velocity mapping. *J. Glaciol.* **2010**, *56*, 415–430.

143. Joughin, I.; Smith, B.; Howat, I.; Scambos, T. *MEaSUREs Greenland Ice Sheet Velocity Map from InSAR Data*; National Snow and Ice Data Center: Boulder, CO, USA, 2010; doi:http://dx.doi.org/10.5067/MEASURES/CRYOSPHERE/nsidc-0478.001.

144. Joughin, I.; Smith, B.; Howat, I.; Scambos, T. *MEaSUREs Greenland Ice Velocity: Selected Glacier Site Velocity Maps from InSAR*; National Snow and Ice Data Center: Boulder, CO, USA, 2013; doi:http://dx.doi.org/10.5067/MEASURES/CRYOSPHERE/nsidc-0481.001.

145. Scheuchl, B.; Mouginot, J.; Rignot, E. Ice velocity changes in the Ross and Ronne sectors observed using satellite radar data from 1997 and 2009. *The Cryosphere* **2012**, *6*, 1019–1030, doi:10.5194/tc-6-1019-2012.

146. Rignot, E.; Mouginot, J.; Scheuchl, B. *MEaSUREs InSAR-Based Ice Velocity Maps of Central Antarctica: 1997 and 2009*; National Snow and Ice Data Center: Boulder, CO, USA, 2012; doi:http://dx.doi.org/10.5067/MEASURES/CRYOSPHERE/nsidc-0525.001.

147. Rignot, E.; Mouginot, J.; Scheuchl, B. Ice flow of the Antarctic ice sheet. *Science* **2011**, *333*, 1427–1430.

148. Rignot, E.; Mouginot, J.; Scheuchl, B. *MEaSUREs InSAR-Based Antarctica Ice Velocity Map*; National Snow and Ice Data Center: Boulder, CO, USA, 2011; doi:http://dx.doi.org/10.5067/MEASURES/CRYOSPHERE/nsidc-0484.001.

149. Rignot, E.; Mouginot, J.; Scheuchl, B. Antarctic grounding line mapping from differential satellite radar interferometry. *Geophys. Res. Lett.* **2011**, *38*, L10504.

150. Rignot, E.; Mouginot, J.; Scheuchl, B. *MEaSUREs Antarctic Grounding Line from Differential Satellite Radar Interferometry*; National Snow and Ice Data Center: Boulder, CO, USA, 2011; doi:http://dx.doi.org/10.5067/MEASURES/CRYOSPHERE/nsidc-0498.001.

151. Kim, Y.; Kimball, J.S.; Zhang, K.; McDonald, K.C. Satellite detection of increasing Northern Hemisphere non-frozen seasons from 1979 to 2008: Implications for regional vegetation growth. *Remote Sens. Environ.* **2012**, *121*, 472–487.

152. Kim, Y.; Kimball, J.S.; Glassy, J.; McDonald, K.C. *MEaSUREs Global Record of Daily Landscape Freeze/Thaw Status. Version 2*; NASA DAAC National Snow and Ice Data Center: Boulder, CO, USA, 2013; doi:http://dx.doi.org/10.5067/MEASURES/CRYOSPHERE/nsidc-0477.002.

153. Zhao, Y.; Liu, A.K.; Long, D.G. Validation of sea ice motion from QuikSCAT with those from SSM/I and buoy. *IEEE Trans. Geosci. Remote Sens.* **2002**, *40*, 1241–1246.

154. Pfeffer, W.T.; Arendt, A.A.; Bliss, A.; Bolch, T.; Cogley, J.G.; Gardner, A.S.; Hagen, J.O.; Hock, R.; Kaser, G.; Kienholz, C.; *et al*. The Randolph Consortium The Randolph Glacier Inventory: A globally complete inventory of glaciers. *J. Glaciol.* **2014**, *60*, 537–552.

155. Remund, Q.P.; Long, D.G. Sea ice extent mapping using Ku band scatterometer data. *J. Geophys. Res. Oceans* **1999**, *104*, 11515–11527.

156. Meier, W.N.; Fetterer, F.; Savoie, M.; Mallory, S.; Duerr, R.; Stroeve, J.C. *NOAA/NSIDC Climate Data Record of Passive Microwave Sea Ice Concentration. Version 2*; National Snow and Ice Data Center: Boulder, CO, USA, 2013; doi:http://dx.doi.org/10.7265/N55M63M1.

157. Hall, D.K.; Salmonson, V.V.; Riggs, G.A. *MODIS/Aqua Sea Ice Extent Daily L3 Global 1km EASE-Grid Day.Version 5*; National Snow and Ice Data Center: Boulder, CO, USA, 2006.

158. Hall, D.K.; Salmonson, V.V.; Riggs, G.A. *MODIS/Terra Sea Ice Extent Daily L3 Global 1 km EASE-Grid Day.Version 5*; National Snow and Ice Data Center: Boulder, CO, USA, 2006.

159. *National Ice Center (NIC) and NSIDC Multisensor Analyzed Sea Ice Extent—Northern Hemisphere*; Developed by F. Fetterer, M. Savoie, S. Helfrich, and P. Clemente-Colón; National Snow Ice Data Center: Boulder, CO, USA, 2010; doi:http://dx.doi.org/10.7265/N5GT5K3K.

160. Fetterer, F.; Knowles, K.; Meier, W.N.; Savoie, M. *Sea Ice Index*; National Snow and Ice Data Center: Boulder, CO, USA, 2002; doi:http://dx.doi.org/10.7265/N5QJ7F7W.

161. Stroeve, J. *Sea Ice Trends and Climatologies from SMMR and SSM/I-SSMIS*; NASA DAAC National Snow and Ice Data Center: Boulder, CO, USA, 2003.

162. National Ice Center; Fetterer, F.; Fowler, C. *National Ice Center Arctic Sea Ice Charts and Climatologies in Gridded Format*; National Snow and Ice Data Center: Boulder, CO, USA, 2009; doi:http://dx.doi.org/10.7265/N5X34VDB

163. Brodzik, M.J.; Armstrong, R. *Northern Hemisphere EASE-Grid 2.0 Weekly Snow Cover and Sea Ice Extent. Version 4*; NASA DAAC National Snow and Ice Data Center: Boulder, CO, USA, 2013.

164. Bindlish, R.; Jackson, T. *Aquarius L3 Gridded 1-Degree Annual Soil Moisture. Version 2*; NASA DAAC National Snow and Ice Data Center: Boulder, CO, USA, 2013; doi:http://dx.doi.org/10.5067/Aquarius/AQ3_ANSM.002

165. Salvatore, M.R.; Mustard, J.F.; Head, J.W.I.; Marchant, D.R.; Wyatt, M.B. Characterization of spectral and geochemical variability within the Ferrar Dolerite of the McMurdo Dry Valleys, Antarctica: Weathering, alteration, and magmatic processes. *Antarct. Sci.* **2014**, *26*, 49–68.

166. Rolstad, C.; Haug, T.; Denby, D. Spatially integrated geodetic glacier mass balance and its uncertainty based on geostatistical analysis: Application to the western Svartisen ice cap, Norway. *J. Glaciol.* **2009**, *55*, 666–680.

167. Kääb, A.; Vollmer, M. Surface geometry, thickness changes and flow fields on creeping mountain permafrost: Automatic extraction by digital image analysis. *Permafr. Periglac. Process.* **2000**, *11*, 315–326.

168. AGU. AGU Publications Data Policy. Available online: http://publications.agu.org/author-resource-center/publication-policies/data-policy/ (accessed on 23 February 2014).

169. Heid, T.; Kääb, A. Evaluation of existing image matching methods for deriving glacier surface displacements globally from optical satellite imagery. *Remote Sens. Environ.* **2012**, *118*, 339–355.

170. Cooper, A.K. Future progress in Antarctic science: Improving data care, sharing and collaboration. *Earth Environ. Sci. Trans. R. Soc. Edinb.* **2013**, *104*, 69–80.

171. Fretwell, P.T.; LaRue, M.A.; Morin, P.; Kooyman, G.L.; Wienecke, B.; Ratcliffe, N.; Fox, A.J.; Fleming, A.H.; Porter, C.; Trathan, P.N. An emperor penguin population estimate: The first global, synoptic survey of a species from space. *PLoS One* **2012**, *7*, e33751.

172. Fretwell, P.T.; Trathan, P.N. Penguins from space: Faecal stains reveal the location of emperor penguin colonies. *Glob. Ecol. Biogeogr.* **2009**, *18*, 543–552.

173. Turner, W. Satellites: Make data freely accessible. *Nature* **2013**, *498*, 37, doi:10.1038/498037c.

174. Meier, W.N.; Gallaher, D.; Campbell, G.G. New estimates of Arctic and Antarctic sea ice extent during September 1964 from recovered Nimbus I satellite imagery. *The Cryosphere* **2013**, *7*, 699–705.

175. Carlson, D. A lesson in sharing. *Nature* **2011**, *469*, 293, doi:10.1038/469293a.